*Annu. Rev. Astron. Astrophys. 1990. 28: 215–61*

# H I IN THE GALAXY[1]

*John M. Dickey*

Department of Astronomy, University of Minnesota, Minneapolis, Minnesota 55455

*Felix J. Lockman*

National Radio Astronomy Observatory, Charlottesville, Virginia 22903

KEY WORDS: galactic structure, interstellar medium, 21-cm radiation, ultraviolet spectra

## 1. PREFACE

This is an observational review. The topic of H I in the Galaxy is so vast that it cannot be covered in any single article. Recent comprehensive reviews by Kulkarni & Heiles emphasizing the thermodynamics and astrophysics of the atomic phase (152, 153), and by Burton on the galactic distribution and morphology of H I (34), together run to more than 120 pages and free us from the burden of discussing those topics here. Instead, we focus on observations of interstellar atomic hydrogen, from Lyman-$\alpha$ and the 21-cm line through indirect tracers like dust and gamma rays; on what one can and cannot learn from these observations; on what the H I sky looks like; and, finally, on the state of our knowledge and prospects for the future. We also discuss results from recent H I studies that bear on two important areas: the spatial organization of interstellar H I, and its vertical distribution in the Galaxy. There is no mention of the galactic nucleus (see 28, 163), and we are unable to summarize or even list the many observations of H I associated with objects such as individual H II regions, supernova remnants, high-velocity clouds, or specific interstellar clouds (see, for example, 56).

The sheer abundance of galactic H I data drives us to speak of it in terms derived from theoretical models that we do not have space to discuss. The temperature variations of the interstellar medium are so dramatic, its

[1] The US Government has the right to retain a nonexclusive royalty-free license in and to any copyright covering this paper.

pressure structure is so problematic, and its dynamics, hydrodynamics, and/or magnetohydrodynamics are so intricate that it has commanded the attention of several generations of the finest theoretical astrophysicists. We assume in this review that the reader is familiar enough with terms like "cloud" and "the two-phase model" to get the gist of what we say, while being thoughtful enough to recognize that, whatever else is true about galactic H I, the last word on its properties has yet to be spoken.

# 2. 21-cm OBSERVATIONS

## 2.1 *Critical Review of the Observational Tools*

2.1.1 GENERAL COMMENTS The only radio transition of ground-state neutral hydrogen is the 21-cm hyperfine line at 1420.4058 MHz. In contrast to the typically highly saturated ultraviolet lines of H I, a Gaussian 21-cm line has an opacity at line center of

$$\tau = 5.2 \times 10^{-19} \frac{N_{\rm H}}{\Delta v T_{\rm s}}, \qquad 1.$$

where the spin temperature $T_{\rm s}$ is the kinetic temperature in most cases, and $\Delta v$ is the line's full width at half-maximum, in kilometers per second (93, 153).

Since typically $T_{\rm s} \geq 50$ K and $\Delta v \sim 10$ km s$^{-1}$, the column density $N_{\rm H}$ must be greater than $10^{21}$ cm$^{-2}$ before the line center is opaque. This is about 10 times the total column density in the direction of the galactic poles (168), but values of $10^{21}$ cm$^{-2}$ in a narrow velocity interval are common at low latitudes or toward dense clouds. So, unlike L$\alpha$, the 21-cm line often has a moderate or even low opacity, and a single spectrum may have a number of line components whose opacities range from $<10^{-4}$ to $\geq 4$. The spectra usually contain a bewildering amount of kinematic detail.

2.1.2 OBSERVING EMISSION Emission at 21 cm was first detected nearly simultaneously by three groups (89, 187), and it was studied intensely in the 1950s by astronomers in the Netherlands and Australia using telescopes of the 25-m class (see ref. 248 for a historical review). The ubiquity of atomic hydrogen in the Galaxy, the low energy of the 21-cm transition, its long lifetime, and its relatively high excitation temperature (compared with the radio continuum brightness temperature in most directions) make it easily detectable in emission in every direction despite its generally low opacity. It is the strongest thermal spectral line in radio astronomy. Profiles have a peak brightness temperature never less than about 0.5 K and as high as 125 K at low galactic latitude.

2.1.2.1 *Sensitivity* The accuracy of galactic 21-cm spectra is not always determined by noise from the receiving equipment. A filled-aperture (single-dish) radio telescope with a state-of-the-art receiver can take spectra at 1 km $s^{-1}$ resolution with a noise level of only $\Delta T_b \sim 0.5\ t^{-1/2}$ K (where $t$ is the integration time, in seconds), independent of the telescope size, structure, or angular resolution. Thus, a minute's integration on a modern single dish gives an H I spectrum with a signal-to-noise ratio of about 15 at the galactic poles and more than 1500 in the plane. Receiver noise is no longer the limiting factor in filled-aperture 21-cm emission studies.

The same is not true for observations using a radio interferometer or "synthetic aperture." Here the noise, expressed as a brightness temperature $\Delta T_b$, depends on the telescope configuration because in these systems it is the noise in units of flux density per beam, i.e. $\Delta T_b \times \text{HPBW}^2$, that is a constant. (HPBW is the full width at half-power of the antenna beam.) In general, a synthesis telescope produces a map that has a brightness noise that goes as the inverse square of the beam size, so increasing the angular resolution of a synthesis telescope by moving the individual elements further apart reduces the telescope's sensitivity to surface brightness. The trade-off is extremely advantageous when observing an object of small angular size and high surface brightness, but it has drawbacks for galactic H I emission work. As an order-of-magnitude example, consider the Very Large Array (VLA), which currently obtains 21-cm spectra with a brightness temperature noise in a 1 km $s^{-1}$ channel of $\Delta T_b \sim 100 \times [\text{HPBW (arcmin)}]^{-2}(t^{-1/2})$ K. In its most compact configuration, the VLA has a HPBW at 21 cm of $\sim 1'$. It would thus take more than 6 hr to get a $3\sigma$ detection on a 1-K galactic H I line from a cloud $1'$ in diameter. At the higher angular resolutions of which the VLA is capable (e.g. $1''$), the integration time required to detect even the bright H I in the galactic plane is prohibitively large.

2.1.2.2 *Stray radiation* Radio telescopes have some response (sidelobes) in all directions, not just in the vicinity of the main beam, and this can compromise H I emission measurements. Sidelobes arise principally from Fraunhofer diffraction at the dish edge and from scattering off the feed-support legs or any other obstacle in the aperture. The aperture-blockage sidelobes, which can lie many tens of degrees off the telescope axis, cause the most problems for galactic H I studies. Although the sidelobes have small amplitude, they cover a large solid angle and can contain a significant fraction of the telescope's total response. When pointed toward the galactic poles, many single dishes receive about equal amounts of radiation from the galactic plane via a far sidelobe as from the pole itself (168). This so-called stray radiation has the effect of reducing the dynamic range of 21-

cm observations and may even create spurious and time-varying spectral features (135).

Stray radiation is not a significant problem for telescopes that have an unblocked aperture, e.g. horns or horn-reflectors, and these have been used to measure highly accurate H I profiles (120, 245, 282). Unfortunately, all existing unblocked telescopes are relatively small and thus have poor angular resolution (HPBW of a few degrees). Larger telescopes can be used for accurate H I studies if their spectra are corrected for stray radiation, either by modeling the sidelobes and compensating for the emission expected in each (135, 267) or by "bootstrapping" observations to those made with unblocked apertures (168). Both methods require substantial off-line computer processing of the data and have been used in only a few directions. The new 100-m class telescope under construction at Green Bank, West Virginia, has been designed to minimize stray radiation and should be a superb instrument for measuring galactic H I.

2.1.2.3 *Aperture synthesis telescopes* Aperture synthesis telescopes have a different sidelobe problem that complicates their use for galactic H I emission studies—namely, the sidelobes are both positive and negative. Because of the very high degree of angular correlation of galactic H I emission, almost all of the signal entering the main beam will be canceled by that which enters nearby negative sidelobes (e.g. 45a, p. 197). This severely reduces the usefulness of most aperture synthesis telescopes for the study of most galactic H I emission unless their data can be combined with accurate single-dish observations to restore the missing signal.

In more formal terms, a multiplying interferometer artificially sets the map average of each spectral channel to zero because it cannot measure the "zero-spacing" flux, i.e. the flux in the *u-v* plane pixel centered on (0, 0). Most galactic H I emission, however, contributes *only* to the (0, 0) pixel and so is absent from the interferometer measurement. Even with perfect knowledge of the sidelobes, the zero-spacing flux still cannot be recovered.

Aperture synthesis radio telescopes are very useful for studying H I emission features of moderate angular size that are isolated, either because they are much brighter than their surroundings or they are at a different velocity than most galactic gas. Examples of these are H I clouds near H II regions, the brighter high-velocity clouds, and, of course, most other galaxies. The unique wide-field aperture synthesis telescope at the Dominion Radio Astrophysical Observatory (Penticton, Canada) is particularly well designed for measuring galactic H I emission. The array consists of small-diameter dishes that allow very short *u-v* spacings to be sampled and also produce maps that cover a wide area (1°.7) at 1′ resolution (e.g. 157, 217a).

2.1.2.4 *State of 21-cm emission surveys* A useful table of the available H I surveys is given by Burton (34). Although every part of the sky has been measured at least once, it is only near the galactic plane that sensitive surveys are complete with $\sim 10'$ angular resolution. Thus, while we know the galactic H I sky well enough to characterize its main features, a researcher looking for a high-quality H I emission spectrum in any given direction may be disappointed with what is available. One problem is that large single-dish telescopes measure 21-cm emission lines no faster than do small telescopes, merely with better angular resolution. Large telescopes have such small beams that it is not feasible to map large areas completely. Also, many existing surveys are compromised by stray radiation at the $\lesssim$1-K level. Much work needs to be done before there is a satisfactory account of the 21-cm sky.

2.1.3 OBSERVING 21-cm ABSORPTION H I viewed against a bright continuum source may appear in absorption. In the simplest general case, the brightness temperature $T_b$ of the 21-cm signal at a velocity $v$, relative to the signal level in the continuum, is a mix of emission and absorption defined by

$$\Delta T_b(v) = [T_s - T_0][1 - e^{-\tau(v)}]. \qquad 2.$$

Absorption dominates emission at velocity $v$ when the brightness temperature of the continuum source averaged over the antenna beam, $T_0$, is greater than the H I spin temperature averaged over the antenna beam, $T_s$, and the optical depth $\tau$ is high. Typically, the emission brightness at a given velocity does not vary strongly with beam size, whereas the observed brightness of a small background continuum source goes as the inverse of the antenna-beam solid angle. In practice, most telescopes measure an average temperature for a point continuum source at 21 cm of $T_0 \sim 100$ $S$(Jy) [HPBW (arcmin)]$^{-2}$. Typical bright extragalactic radio continuum sources are several janskys, and the smallest beam that one gets from a single dish is about 3.′2 at Arecibo, so except in a few special directions $T_0$ is at most several tens of kelvins. This is smaller than the typical values of $T_s$. Single dishes, then, generally measure a net H I emission profile even when pointed at a relatively bright continuum source, albeit an emission profile that has been reduced somewhat by absorption.

To untangle $\tau(v)$ from Equation 2 and thus obtain the average kinetic temperature and column density as a function of velocity, it is necessary to determine what the emission would be in the absence of a continuum source by one of two techniques: (*a*) use a variable continuum source, such as a pulsar, as a target and measure the pure emission term when the source is "off"; or (*b*) observe the H I emission in directions near the

continuum source and interpolate an "expected" emission profile toward the source.

Observation of 21-cm absorption against pulsars is quite difficult because the typical pulsar is weak at 21 cm ($S \ll 1$ Jy). As a result, most spectra are noisy and only a small fraction of all pulsars have been observed (49). Nonetheless, the results have special value because of a pulsar's extremely small angular size, which probes the narrowest possible line of sight. The observations have also helped establish distances to pulsars and thus map the galactic electron distribution using the pulsars' dispersion measures (278).

2.1.3.1 *Single-dish absorption studies* Even the largest single dish rarely measures a net absorption spectrum [i.e. $\Delta T_b(v)$ is usually positive], so the accuracy of the observations depends on the accuracy with which the expected emission profile can be determined. Natural emission fluctuations across the sky *always* dominate the error budget of the resulting absorption spectrum. The rms uncertainty of spectra from the Arecibo telescope is typically $\sim 0.5$ K at moderate galactic latitude, which is greater than the noise in a spectrum for integration times longer than a few seconds; it may rise to $\gtrsim 2$ K at low latitudes. This spectral-line confusion appears only at velocities where real emission is present, so the reliability of an absorption spectrum cannot be estimated from the spectral baseline away from the line. The accuracy of the absorption spectrum is a strong function of telescope size. The smaller the telescope, the larger is its beamwidth, so not only is the absorbing component of Equation 2 weaker, but the reference spectrum must be taken farther from the continuum source, where it is less likely to be representative of the "on" position. Liszt (162) has argued from simulations that a telescope must be $> 100$ m in diameter to produce a trustworthy absorption spectrum, except for the strongest continuum sources ($> 10$ Jy). Ironically, the emission fluctuations, or noise of any sort, limit the measurement of high-opacity lines more than that of optically thin lines because the "optical depth noise" goes as $\Delta\tau = \sigma_\tau \times e^\tau$. Additional discussion of the observational techniques is given by Colgan et al (50).

2.1.3.2 *Absorption studies using interferometers* Interferometers can have higher angular resolution than any single dish, and most background continuum sources are well matched to their angular response. For example, the VLA in the "A" configuration has a beam of $\sim 1''$ at 21 cm, so a 1-Jy point source has an average brightness over the beam of $\sim 5 \times 10^5$ K, whereas the receiver noise in the spectrum is two orders of magnitude smaller after only an hour's integration. Absorption lines with $\tau \gtrsim 0.1$ are detected easily, but the emission, even if it has a $T_b \sim 100$ K, is below the

noise level. In addition, the negative sidelobes of an interferometer, which interfere with its ability to measure H I in emission, are an asset for absorption measurements because they further diminish the smooth emission component that varies slowly across the sky. Recent studies have used aperture synthesis instruments to generate a very small, clean beam and measure absorption toward compact sources (78) or map the distribution of absorption across the face of an extended background source (60, 105).

Although interferometers reject the bulk of the 21-cm emission, there is still the potential for confusion if the emission has some structure on angles as small as the fringe separation for some or all of the baselines used in the aperture synthesis. At low latitudes, even baselines as long as 1 km (fringe separation 44″) can show traces of galactic emission. Since the amplitude of the emission fringes decreases roughly as the angle to the power two to three (59), and the brightness of the absorption goes as the inverse beamwidth squared, the ultimate absorption sensitivity that a telescope can achieve is proportional to its angular resolution to about the fourth power.

The telescope dynamic range sets a limit on the maximum absorption sensitivity also, since at some level the absorption spectra toward nearby continuum sources blend with the spectrum toward the source of interest. If the absorption is different toward different continuum sources in the field, there will be errors at the level of $\Delta\tau/R$, where $\Delta\tau$ is the variation in optical depth over the field and $R$ is the dynamic range (typically 100 to 1000 or more for well-calibrated observations).

Observational techniques for synthesis telescope observations of 21-cm absorption are discussed by van Gorkom & Ekers (266). The experimental results can be particularly sensitive to details of these techniques, especially if the background continuum source is extended. For example, if individual channels are "cleaned" separately before subtracting the continuum, spurious variations in optical depth may be generated. Also, variation in the surface brightness of the background continuum source causes even a constant level of noise in channel maps to generate a wildly varying noise level in $e^{-\tau}$ and in $\tau$.

As an example of what is currently possible, it takes about 4 hr at the VLA to obtain a spectrum with optical depth noise $\sigma_\tau \sim 0.1$ at a velocity resolution of 1 km $s^{-1}$ toward a 50-mJy source. It is impractical to go much deeper in optical depth, or to get a spectrum with even such meager sensitivity toward a much fainter background source, because the telescope time required soon becomes prohibitively large. But since there is typically one extragalactic background source per square degree with $S \gtrsim 50$ mJy, it should be possible to obtain an absorption spectrum within a degree or so of any direction of interest. This will be adequate for many purposes

because there is usually a fair correlation between absorption spectra separated by a degree or less at high and intermediate latitudes.

2.1.3.3 *Absorption surveys* The first observations of 21-cm absorption were made by Hagen et al (107) toward very strong galactic continuum sources using a single-dish telescope, followed by Muller (186) and Shuter & Verschuur (235), but after that until the mid-1970s most advances in absorption studies were made by interferometers at Caltech (46, 47, 127) and at Parkes (207). Further single-dish absorption studies became possible when instruments of the 100-m class became available (69, 180, 281). In particular, the Nançay radio telescope, because of its special geometry, is particularly suited for absorption studies (61, 137, 158). The upgraded Arecibo telescope has been used for these observations since the late 1970s (50, 62, 79, 80, 148, 197–199, 237). In addition, combined observations using interferometers to measure the absorption and single dishes to measure the emission have been done at the Parkes Radio Observatory and at Green Bank (44, 75, 100, 181, 209, 210, 216). More recently, there have been several absorption studies using the VLA (78, 97), the Arecibo interferometer (156), and the Ratan 600 telescope (2). About 500 absorption spectra are now available with sensitivity to $\tau \gtrsim 0.1$; some 50 to 100 have sensitivity to lines a factor of 3 to 10 weaker.

2.1.3.4 *VLBI* Absorption by the 21-cm line can be measured and even mapped at an angular resolution of $\leq 0\farcs1$ using VLBI techniques if the background continuum source is suitable. Dieter et al (81) did the first successful experiment of this kind and detected a surprisingly strong variation in the optical depth of absorbing gas in front of 3C 147 over about $0\farcs2$. On this line of sight this corresponds to a linear size of 70 AU or less. This result has recently been confirmed by Diamond et al (73) using the European VLBI Network; similar small-scale structure is suggested in two other directions.

These results are stunning, particularly since the background sources used are extragalactic, so the directions studied should give random samples of low-latitude interstellar gas. The column density needed for the absorption is a few times $10^{19}$ cm$^{-2}$, which implies a volume density of nearly $10^5$ cm$^{-3}$ if the optical depth variation is caused by density change alone. Whether these are distinct structures or some sort of discontinuous internal variations in the density and/or temperature inside larger clouds is not yet known. If they are discrete structures, they need contain only $10^{-8}$ $M_\odot$. The highest resolution VLA maps of absorption toward Orion (262) also show very small concentrations of gas. However, with sizes of a few tenths of a parsec and masses typically of 0.01 $M_\odot$, these subparsec clouds are vastly larger and more massive than those found by the VLBI

experiments. Both may be the result of the passage of a shock front through a much larger cloud. The recently discovered structure in the ionized medium on scales of $\sim 10$ AU (92c, 281a) might be related to the small-scale structure in the cool neutral medium if, for example, both are caused by instabilities behind supernova shocks, but this connection is only speculative.

2.1.4 OBSERVING SELF-ABSORPTION Just as interstellar Lα absorption can be detected against the broad Lα emission lines from late-type stars, so too can a cold H I cloud appear in absorption against H I emission from warmer gas behind it. Two circumstances are illustrated in Figure 1, along with the 21-cm profiles that result: The telescope on the left measures the sum of the two profiles because the hot cloud is optically thin, and the telescope on the right sees a self-absorbed profile.

Self-absorption was first detected against the low-latitude, bright H I toward the galactic center and anticenter (109, 205). Its occurrence is direct evidence that the kinetic temperature of galactic H I has a large range.

The phenomenon can be difficult to recognize in a complex spectrum, and Knapp (144) has proposed that self-absorbed features be identified by

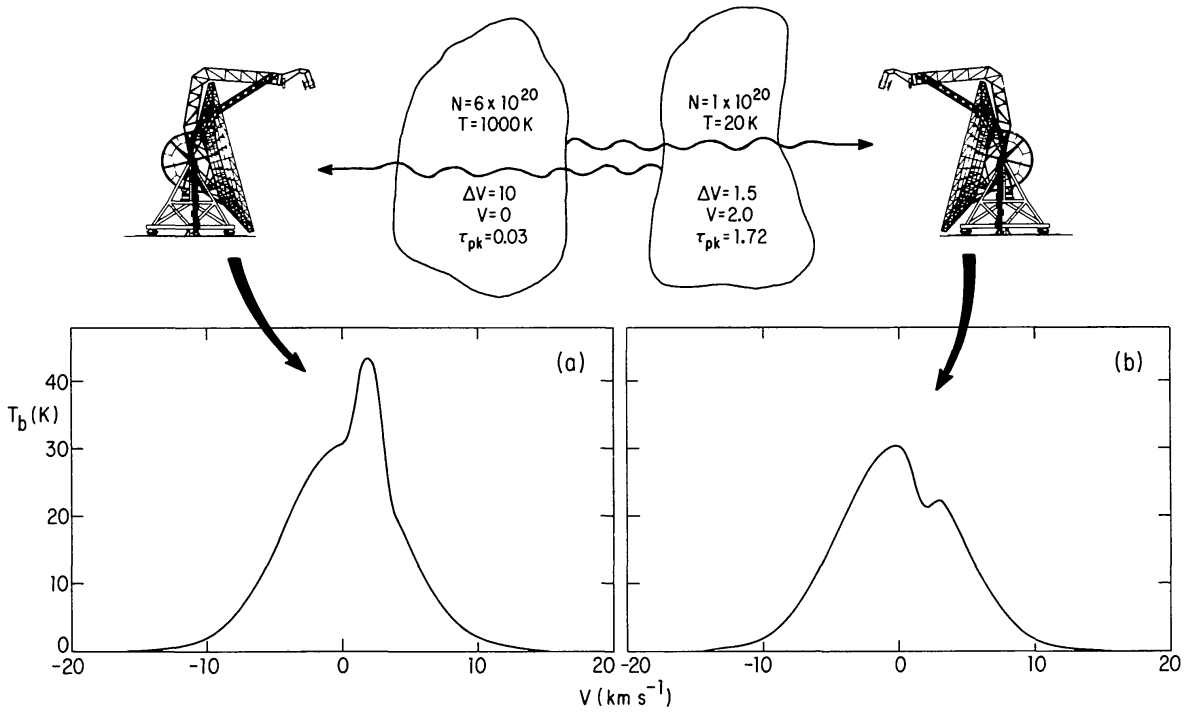


*Figure 1* Schematic of the geometry of 21-cm self-absorption. The structure of an emission profile depends on the relative location of hot and cold clouds as viewed by the observer. Superpositions like this are very common at low and intermediate latitudes. The profile on the right (*b*) is self-absorbed.

the following characteristics: (*a*) They should have a relatively narrow line width of only a few kilometers per second, implying that the kinetic temperature is low; (*b*) they should have steep sides, so that they are unlikely to be just the chance sum of emission components; and (*c*) they should be relatively localized in space. A self-absorption feature is also suspected where a sharp minimum is seen in an H I emission profile at the velocity of a molecular cloud in the same direction. Conditions for observable self-absorption are most favorable at low galactic latitudes, where the H I is fairly bright, or in the direction of local gas clouds that subtend many arcminutes. The technique is useful for determining cloud properties in directions lacking suitable background radio continuum sources (5, 8, 37, 178, 220, 222, 234).

In analyzing a self-absorbed profile, such as Figure 1*b*, one usually estimates the background emission by drawing a smooth curve connecting the apparently unabsorbed portions of the spectrum. This step introduces considerable uncertainty, especially for complex spectra (159), and still leaves two unknowns (the spin temperature and the opacity of the cloud) and only one measured quantity ($\Delta T_b$). The ambiguity can be resolved if the cloud covers so large an angle that one can literally move off the background H I, as one moves off a background continuum source, and obtain a pure emission profile for the cloud. Circumstances like this are more common than one might expect (206). At least one cloud goes from emission to self-absorption as it crosses the bright H I in the galactic plane (9), and van der Werf et al (261) have observed a cloud that appears in self-absorption at its center but in emission at its edges. Where the cloud disappears, its spin temperature must be close to the brightness temperature of the background H I, in this case about 25 K.

Most self-absorption studies, however, can give only a range of temperature and density for the absorbing cloud, usually with significant uncertainty. Although the range can be restricted in some cases (219), there is little or no way to determine a confidence level for an individual measurement of $\tau$.

It is possible that self-absorption causes much of the structure in low-latitude galactic emission profiles. Prominent examples of self-absorption remain a sobering reminder that there are places in the interstellar medium where the 21-cm brightness decreases as the H I column density goes up.

2.1.5 COLUMN DENSITY MEASUREMENT One of the major deductions from 21-cm observations is the total column density of H I, or the column density at a particular velocity or in a particular spectral component. If the 21-cm line is optically thin in the direction of interest, then the column density is given by the velocity integral (in K km $s^{-1}$) under the profile:

$$N_{\rm H}(\tau \ll 1) = 1.823 \times 10^{18} \int T_{\rm b}\, dv\, {\rm cm}^{-2}. \qquad 3.$$

Given only an emission spectrum and not a measurement of $\tau$ itself, a reasonable rule of thumb is that if the peak $T_{\rm b}$ is only a few tens of kelvins or less, the optically thin assumption is probably not too bad. Most H I is hotter than 20 K, so a peak $T_{\rm b}$ less than that suggests a modest opacity if self-absorption and other evidence of cool gas are absent.

A first-order opacity correction can be made by adopting a constant $T_{\rm s}$ for a spectrum. Most large-scale emission surveys have been analyzed this way using values of $T_{\rm s}$ in the range 120–150 K (e.g. 35, 143, 194).

If the 21-cm line has significant opacity, a unique interpretation of the data is usually impossible because a cloud with an optical depth $\tau$ greater than a few tenths partially obscures the emission from gas behind it. At the velocity of this cloud, the emission brightness temperature is a function of the spin temperature and optical depth of the cloud, plus the column density of any foreground optically thin gas and the attenuated column density of the background gas. Even with both emission and absorption observations, and thus a measurement of $\langle T_{\rm s} \rangle$ and $\langle \tau \rangle$ at each velocity, there is no unique $N_{\rm H}(v)$, since correction for opacity depends on the detailed juxtaposition of warm and cool gas. The algebra of this radiative transfer problem is discussed by many authors (50, 75, 153). As an example, consider the spectra in Figure 1. The optically thin assumption gives an $N_{\rm H}$ that is 10% too low for spectrum (*a*) and 20% too low for spectrum (*b*). The assumption that the gas is isothermal at 125 K gives an $N_{\rm H}$ that is only 5% too high for (*a*) but 10% too low for (*b*).

The need to correct for opacity in 21-cm profiles ultimately limits the accuracy of many $N_{\rm H}$ determinations (88). In most directions, the total column density derived from an optically thin analysis of an emission spectrum should be multiplied by factors of 1.1–1.3 to account for self-absorption. There are, however, a few places where the factor gets large as cold clouds shield a region of velocity crowding. Observation of 21-cm absorption toward extragalactic continuum sources and other evidence (200) shows that considerably less than half of all velocities in low-latitude spectra are covered by H I with $\tau > 1$. While opacity effects make it difficult to derive a very accurate $N_{\rm H}$ at low galactic latitude ($|b| \lesssim 10°$), it is unlikely that 21-cm emission surveys have missed more than about 20–30% of the mass of galactic H I, on average (80a).

2.1.6 THE ZEEMAN EFFECT AT 21-cm The line-of-sight component of the interstellar magnetic field shifts the frequency of the two circular polarizations of the 21-cm line by a small amount. This effect was first detected

by Verschuur (269). There have been several recent comprehensive reviews of Zeeman observations along with other methods for measuring the interstellar magnetic field (115, 152, 254, 256).

2.1.6.1 *Observational considerations* The Zeeman effect is extremely difficult to measure at 21 cm, not only because very high sensitivity is needed to achieve even a significant upper limit, but because of the subtle calibration required and the many sources of spurious polarized signals that mask and even mimic the effect. High sensitivity is necessary because the frequency difference between the two polarizations is very small, only 2.8 Hz $(\mu G)^{-1}$, so that for the typical interstellar field strength of a few microgauss the splitting is more than two orders of magnitude smaller than the H I line width. Thus, rather than seeing separate lines in the two polarizations, one sees at best an almost imperceptible shift in the line center. This is generally measured differentially—for example, using a switch that synchronously subtracts the signals from two circularly polarized feeds (254).

Zeeman splitting can be observed in emission or in absorption. The former technique benefits from the strength of the lines on even a small telescope, whereas the latter has the advantage of narrower lines and a sampling of a more restricted volume in space that reduces the possibility that the effect will be canceled by a reversal of the magnetic field along the line of sight. But even with a relatively strong $B_{\|}$ of 10 $\mu$G, the amplitude of the circular polarization differential signal is only $10^{-3}$ of the total brightness in emission, and perhaps 3 times that in absorption. Thus, to detect the Zeeman splitting takes about $10^6$ times longer than the time required to detect the line itself.

2.1.6.2 *General results* Most recent observations of the Zeeman effect in 21-cm emission have been made with the 25-m telescope at the Hat Creek Observatory (reviewed by Heiles in ref. 115; see also 116a, 117, 271). This telescope has been carefully calibrated in circular polarization, and integration times of many days per spectrum have been achieved. Because of the enormous time and effort needed to obtain a good measurement, the body of existing data is neither large nor systematic. It consists mainly of observations in "interesting" directions.

Measured field strengths typically range from $\sim$10 to $\sim$100 $\mu$G and vary considerably and to some extent unpredictably from point to point. The magnetic field seems to be concentrated in filamentary structures that lie on the surfaces of H I shells and supershells. This concentration may be the result of the interstellar shocks associated with the shells. The magnetic field pressure $P/k$ is typically several times $10^4$ cm$^{-3}$ K, which is much larger than the thermal pressure in the H I gas (typically 2–3 $\times$ $10^3$

$cm^{-3}$ K) and larger than the equivalent pressure in macroscopic and turbulent motions (typically 2–5 times the thermal pressure) indicated by the 21-cm line width. It is tempting to associate these line widths with Alfvén waves (92) and consider the macroscopic motion of the gas to be a response to magnetic pressure gradients resulting from the field configuration (117). The magnetic field evidently dominates the small- and intermediate-scale kinematics of interstellar H I in many regions. In one interpretation (56), the magnetic field can also moderate the response to thermal instabilities in the neutral gas and so determine the thermodynamic phase balance in interstellar H I. On the other hand, many directions have upper limits to the magnetic field of 3–5 $\mu$G or less. These areas, where the magnetic pressure is less than or comparable to the pressure due to macroscopic motions, are probably more typical of interstellar H I as a whole than those exceptional regions of strong fields that give the positive detections of Zeeman splitting.

In 21-cm absorption, few regions have been well observed because of the long integration times needed even to place interesting limits on the field strength. Detailed maps of the field distribution toward the very bright supernova remnant Cas A have been made with the Westerbork synthesis telescope (24, 229). In one spectral feature the magnetic field strength more than doubles, from 20 to 50 $\mu$G, over a distance of 4 pc. The regions of higher magnetic field strength correspond with the position of molecular clumps embedded in the cool H I cloud (253). Recent VLA studies of the 21-cm Zeeman effect in Orion (257, 262) and W3 (263) show again that the magnetic pressure is sufficient to overcome gas pressure, bulk motions, and gravitational forces in large areas around these H II regions. Small-scale structure is seen in the field configuration with reversals over lengths less than 1 pc, suggesting a tangled field. This may be the result of the recent nearby star formation.

On larger scales the existence of a correlation between field strength and gas density in the atomic phase is tentative (254–256), although strong fields are seen in the 18-cm lines of OH, originating where the density is several hundred atoms per cubic centimeter or higher (64, 191, 253).

Although interest in measuring 21-cm Zeeman splitting is increasing and more telescopes are being used to measure the effect, we still know less about the strength and direction of the magnetic field than about any other major aspect of galactic H I. This area of research is ripe for observational advances.

## 2.2 *General Characteristics of 21-cm Observations*

All 21-cm spectra, despite their diversity, have a number of common attributes, which are illustrated in Figures 2 and 3. The data in Figure

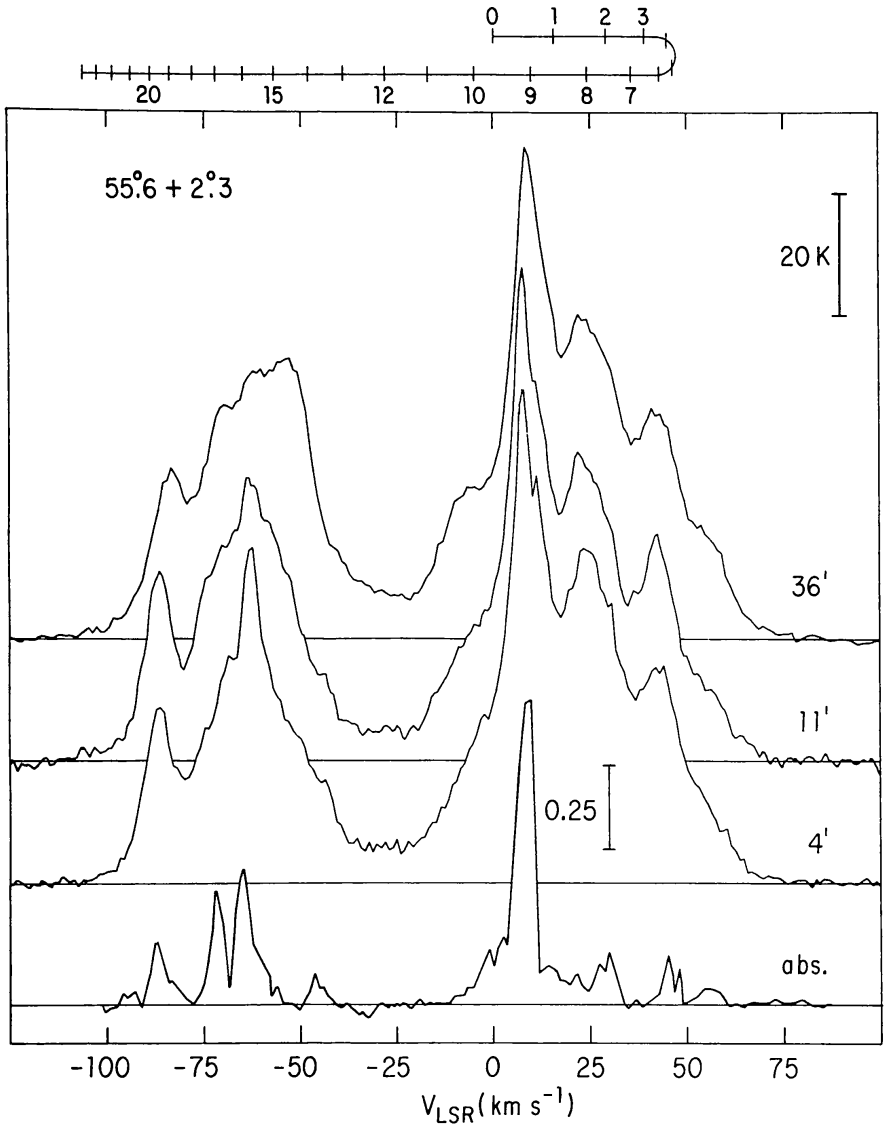


*Figure 2* Representative 21-cm emission and absorption profiles at low galactic latitude. All are in the same direction $(l, b) = (55°.6, +2°.3)$. The emission profiles were taken with angular resolutions of 36′, 11′, and 4′, while the absorption is measured against an extragalactic source that subtends $<0'.1$ (9, 78, 277). The emission profiles are in brightness temperature on the scale given by the bar labeled "20 K." The absorption profile (inverted here) gives the value of $1-e^{-\tau} \sim \tau$ at each velocity, and its reference bar has $\tau = 0.25$. At the top of the figure is a curve that shows the relation between velocity and distance from the Sun (in kiloparsecs) for an assumed galactic rotation law (36). While there are only minor differences among the emission profiles despite the differing angular resolution, the absorption profile looks quite different. This is not an effect of angular resolution but of the bias of absorption spectra to the coldest H I.

2 were taken near $(l, b) = (55.^{\circ}6, +2.^{\circ}3)$ in emission at several angular resolutions and in absorption against an extragalactic continuum source that has an angular size of $<0.''1$. The curve at the top of the figure shows how the velocity, if interpreted entirely as galactic rotation, corresponds to distance from the Sun [using a rotation curve (36) scaled to $R_0 = 8.5$ kpc]. Positive velocities imply galactocentric radii $<8.5$ kpc, i.e. within the solar circle. This particular line of sight intersects the galactic "disk" twice: first near the Sun, then again as it passes through the galactic warp more than 15 kpc from the Sun and $>500$ pc above the nominal galactic plane. The relatively bright and complex emission at negative velocities comes from the galactic warp. Emission spectra with this sensitivity can be obtained in about 1 min with current receivers. The absorption spectrum was obtained in 1 hr using the VLA.

Low-latitude emission spectra, such as those shown here, are always very complex; the signal commonly extends over several hundred kilometers per second. The shape of the emission spectra does not change greatly with angular resolution in the inner Galaxy (6), which here lies at positive velocities. Except for self-absorbed features, high-angular-resolution observations near the plane have revealed surprisingly little not already seen in lower resolution observations. This relative absence of angular structure is caused in part by "velocity crowding," a term first used by Burton (32) to emphasize the fact that galactic rotation, projected on the line of sight, often does not impart very much of a velocity difference to spatially separated objects. A long distance can be "crowded" into a small velocity interval. On Figure 2, for example, the velocities from 20 to 30 km $s^{-1}$ cover $>1.5$ kpc. When a lot of space is squashed into a few kilometers per second, individual interstellar components blend completely, and little structure is revealed by increasing the angular resolution except, perhaps, for an occasional cold foreground cloud that can appear in self-absorption. The absence of significant small-scale angular structure at positive velocities is not the consequence of opacity of the line: The absorption spectrum clearly shows that the gas is optically thin at most velocities.

Small-scale angular structure in the negative velocity emission of Figure 2, e.g. near $-65$ km $s^{-1}$, arises because this gas is so distant that the $36'$ beam covers 160 pc, which is comparable to the size of major structures in the interstellar medium (ISM), and even to the thickness of the H I layer.

The overall shape of the emission profiles in Figure 2 is mainly determined by the large-scale distribution and kinematics of H I in the Galaxy. The bright, low-velocity gas is local, and the emission diminishes with distance as the line of sight gets farther from the galactic plane. H I profiles

at low galactic latitude always have several distinct peaks. The origin of these is somewhat controversial; they are manifestations of variations in velocity crowding as well as genuine density enhancements (33, 34). Large features in "longitude-velocity" space are seen in both 21-cm and CO surveys (33), but their identification with spiral arms or "superclouds" is ambiguous (87).

The picture in H I absorption is substantially different from that in emission. The quantity plotted in Figure 2 is the fractional absorption $(1-e^{-\tau})$, which (unlike the emission) varies strongly with the gas temperature. Absorption lines are always narrower than emission lines. Absorption near the plane is common but highly variable. Some velocities have H I emission but no detectable H I absorption. For example, there is often little or no absorption between major emission peaks, whereas all allowed velocities always show significant H I emission. There was dispute for some time over whether this effect could be caused by the different solid angles of the absorption background source and the telescope beam used to measure emission (e.g. 104). However, with the introduction of smaller beams and large absorption surveys the explanation has been convincingly shown to be that suggested originally by Clark (46)—i.e. that the difference between emission and absorption results mainly from variation in the spin temperature of the H I along the line of sight.

The absorption spectrum of Figure 2 is not particularly rich in individual features. To some extent it suffers from the same latitude influence as the emission spectra: H I far from the galactic plane usually has a smaller opacity than that close to the plane (154). But once the sight line pierces the galactic warp, at negative velocities, absorption is again seen. It is interesting to note that cool H I clouds are found even 15–20 kpc from the galactic center.

Unlike emission spectra, which do not look like the superposition of a few Gaussians with unambiguous line centers and widths, absorption spectra can usually be decomposed into Gaussian components, although it may be difficult to extract the weakest lines from a blend. In comparison with 21-cm emission, it is surprising how nearly Gaussian most absorption features are. This is because the absorption lines arise only in regions of cool gas, which are more distinct along the line of sight, and which have narrower intrinsic line widths, than the gas that contributes to H I emission.

Emission at high latitudes is typified by the spectrum in Figure 3, which is in the direction of the radio galaxy 3C 287. Sensitive observations have detected no 21-cm absorption in this direction, implying that the peak 21-cm opacity is less than 1% (80). It is common for there to be little or no H I absorption in directions with $|b| \gtrsim 45°$.

H I emission profiles are never simple, single Gaussians; virtually all

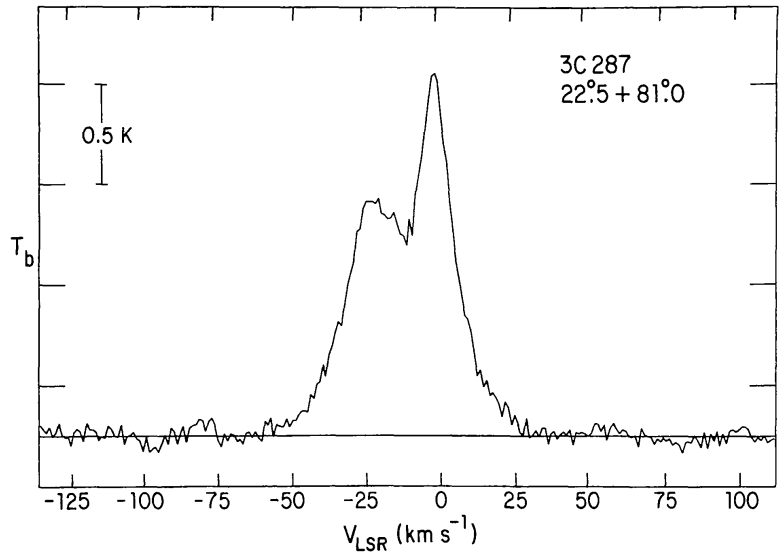


*Figure 3* A representative 21-cm emission profile at high galactic latitude. This profile is toward the radio source 3C 287. No H I absorption has been detected in this direction, which implies that $\tau < 0.01$. Multiple spectral components, often with different velocities, are common in galactic H I profiles, even at high latitude. The component at $-25$ km $s^{-1}$ is an example of the apparently infalling gas that is widespread at northern latitudes (80b, 279; see also Section 6.1).

show multiple components, line asymmetries, or broad wings. Sometimes, as in Figure 3, they contain components whose velocity cannot arise from galactic rotation. It is not generally useful to try to decompose emission spectra into Gaussian components because a profile's shape is determined as much by the vagaries of galactic rotation, velocity crowding, and streaming, modified by opacity and variations in temperature, as it is by the superposition of discrete elements. A Gaussian analysis provides unambiguous information only when an emission feature has a very odd velocity (such as high-velocity clouds) or is very much brighter than its surroundings, so that it is not blended with most other emission.

## 2.3 *Integral Properties of the H I Sky*

Some fundamental aspects of the H I sky can be seen in the distribution of total column densities; thanks to a number of recent surveys (38, 48, 130, 141, 245, 277), reasonably accurate data are available. The following discussion is based on these surveys merged and averaged into $1° \times 1°$ bins in $l$ and $b$; this gridding is adequate for most purposes, except near the galactic plane. Column densities were calculated for $T_s = 200$ K and include all emission within $\pm 250$ km $s^{-1}$ of zero velocity (LSR), except for that associated with the Magellanic Clouds.

The total H I column density varies by a factor of at least 500 across

the sky. The location of the highest $N_H$ is not well known because of opacity effects; the highest value in our data set, $2.6 \times 10^{22}$ cm$^{-2}$ at $(l, b) = (339°, 0°)$, is certainly less than the true maximum. The lowest column density, however, has been fairly well established as $4.4 \pm 0.5 \times 10^{19}$ cm$^{-2}$ at $(l, b) = (152°, +62°)$ in Ursa Major (130, 168). Toward the galactic poles, the column density is $\sim 10^{20}$ cm$^{-2}$.

The frequency of occurrence of a given column density is shown in Figure 4. The general form of this figure, with its steep decrease at the low-$N_H$ end, and the long tail to high $N_H$, would be seen in any uniform H I disk observed from within, but the large breadth of the distribution indicates that there are substantial variations in $N_H$ at all latitudes. The cutoff below $N_H \sim 10^{20}$ is real and not an artifact of limited sensitivity or stray radiation.

The distribution of $N_H$ with latitude shown in Figure 5 is dominated by the galactic plane, which has a FWHM of about 4° on average. As mentioned above, the values of $N_H$ in our data set span a range of $> 500$, but most of this is a csc $|b|$ effect. The actual deviations from a simple plane-parallel layer are shown in Figure 6, where $N_H \sin |b|$ is plotted against $\sin |b|$. These column densities vary by a factor of $\sim 10$ owing in part to several large H I concentrations (e.g. in Orion and Taurus) that lie far from the plane. The fact that $N_H \sin |b| \to 0$ as $\sin |b| \to 0$ is mainly a

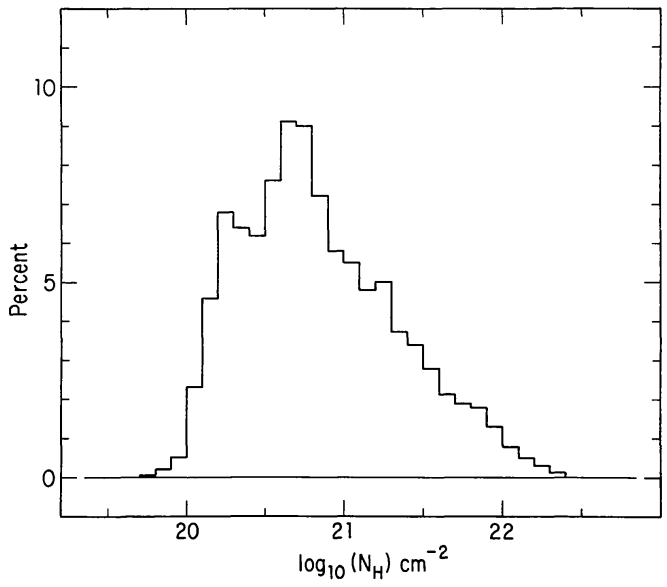


*Figure 4* The percentage of the sky covered by H I at a given $N_H$. Each column density has been averaged over 1° × 1°. This figure is somewhat incomplete at the high-$N_H$ end but should otherwise be representative. It was derived using data and assumptions described in Section 2.2. The same data set is used for Figures 5–8.

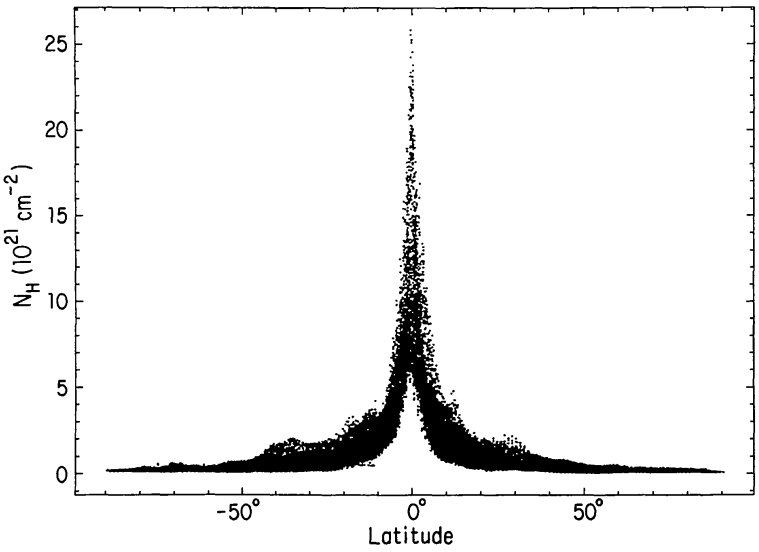


*Figure 5* H I column densities, each averaged over 1° × 1°, versus galactic latitude for the entire sky.

consequence of the finite size of the galactic disk, although opacity effects and the grid size also contribute somewhat.

The data in Figure 6 (for $|b| > 2°.5$) have a mean of $2.9 \times 10^{20}$ csc $|b|$ and a dispersion of $1.4 \times 10^{20}$ cm$^{-2}$. These values are consistent with other determinations of $\langle N_H \rangle$ (145, 162). The mean, however, changes with latitude in a systematic deviation from a uniform plane-parallel layer (145).

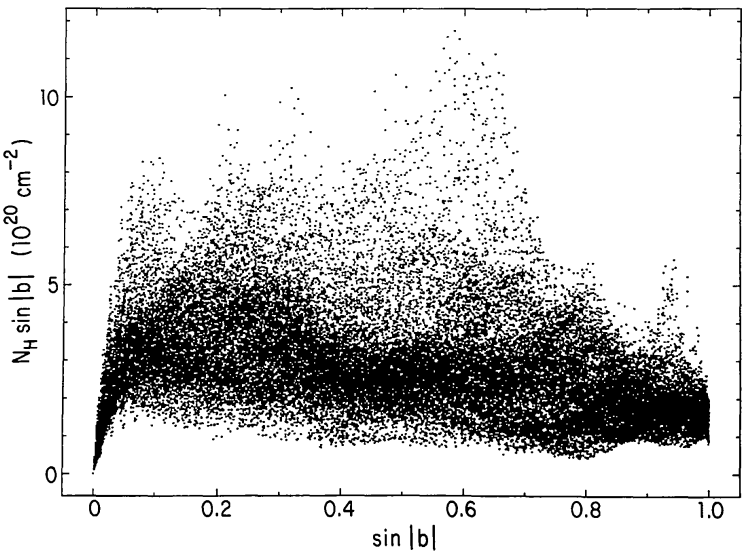


*Figure 6* H I column densities multiplied by sin $|b|$ and plotted versus sin $|b|$ for the entire sky. They go to zero as the latitude goes to zero, mainly because the Galaxy has a finite size. The decrease in $\langle N_H \sin|b| \rangle$ at high latitude is an effect of the hot cavity in the interstellar medium that extends some 100 pc around the Sun.

A fit to the binned median of the distribution gives $N_H = 3.84 \csc |b| - 2.11$, in units of $10^{20}$ cm$^{-2}$. More than two thirds of the points lie within $1.0 \times 10^{20} \csc |b|$ of this line. The minimum $N_H$ does not lie at the poles but near $b = +55°$.

The decrease in $N_H \sin |b|$ at high latitudes is a consequence of the Sun's location in a very low density region of the interstellar medium (reviewed in ref. 57). A number of supernovae have apparently excavated an irregular cavity 100–200 pc in diameter in which the Sun resides. The cavity contains little H I but is filled with low-density, fully ionized gas that radiates in the soft X-ray bands. The vertical extent of the excavated region is comparable to the usual vertical thickness of the H I layer, so the high-latitude H I sky has been perturbed substantially by this event. This is discussed in detail by McCammon & Sanders (177a) elsewhere in this volume.

The H I sky is shown in Figure 7. The top panel gives the total $N_H$, while the bottom panel gives $N_H \sin |b|$ and therefore the deviations of the sky from a uniform plane-parallel system. The regions of excess $N_H \sin |b|$ often lie in arching filaments, some associated with well-known structures like the North Polar Spur and the shell around the North Celestial Pole (135°, +35°). These are no doubt regions like our own local cavity, though in many cases more vast, that have been arranged by a series of supernovae. Pictures like this have led to suggestions that the organization of interstellar H I is better described with words like "sheet" or "filament" than the more usual "cloud" (111). We discuss this topic in Section 5.

The southern galactic sky ($b < 0°$) has about 20% more H I than the northern sky. This is partly due to a large tongue of H I that extends south in the anticenter, but the phenomenon is more general: There is more H I in the south than in the north at all latitudes. This may be another effect of the local cavity (57), for high-latitude molecular clouds have a similar asymmetry (174).

## 3. ULTRAVIOLET OBSERVATIONS

The Lyman series of H I transitions lies in the ultraviolet between 1216 and 912 Å and cannot be observed from the ground. Diffuse L$\alpha$ emission from backscattered solar radiation has been studied to obtain information on the neutral interstellar medium surrounding the Sun (12), but the biggest contribution of ultraviolet observations to the study of galactic H I has come from the Lyman series of lines measured in absorption against background targets, mainly stars (see the reviews in refs. 54, 243). The first measurements of interstellar L$\alpha$ absorption were made from sounding rockets (43, 185). Observations have now been made toward about 300

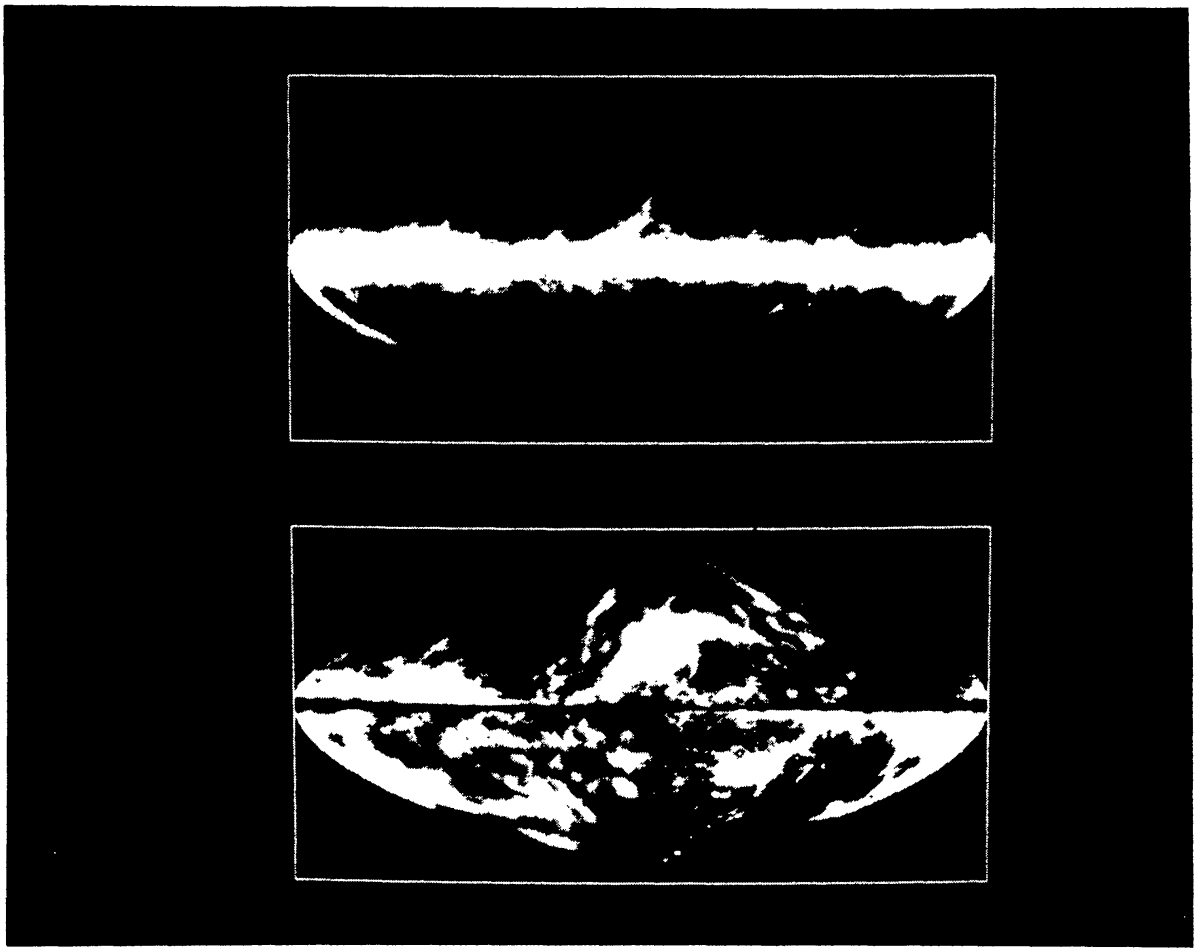

*Figure 7* Two views of the H I sky. Both maps are centered on the galactic center with longitude increasing to the left. (*Top panel*) The distribution of total H I column densities. (*Bottom panel*) The distribution of $N_H$ sin $|b|$. This shows the deviation of the sky from a uniform, infinite, plane-parallel layer. The loops and arching filaments have probably been swept up by supernovae.

stars from the space observatories *OAO-2* (224), *Copernicus* (20), and *IUE* (233). The Hubble Space Telescope (HST) is intended to be the next in this series of observatories.

Lyman-$\alpha$ at 1216 Å is the strongest interstellar absorption line. It is saturated in almost all directions and thus it does not yield radial velocities, but conversely it does give a fairly accurate column density. Equivalent widths are derived by fitting model profiles to the observed spectra (226, 233); column densities have uncertainties in the range 10–40%. Currently the major source of uncertainty in a derived $N_H$ comes from errors in the estimated stellar continuum; new instruments to be launched in the next decade should reduce the total error to $<10\%$.

Most targets for Lα absorption measurements are early-type stars of spectral class no later than B2. Stars of later spectral class have strong stellar Lα absorption lines that contaminate the interstellar lines. The dividing line between useful and suspect types, although generally placed at B2, is not always precise, for it depends somewhat on the interstellar H I column density (226). Early-type stars are so intrinsically luminous that Lα observations have ample sensitivity despite the relatively small aperture of the telescopes that have flown thus far. For example, the *IUE* has detected interstellar Lα absorption toward unreddened B0V stars as faint as $m_V = 12$–13 (223), which corresponds to distances of up to $\sim$20 kpc. This sensitivity is sufficient to detect Lα absorption toward nearly every early-type star that is at moderate and high galactic latitude. The increased sensitivity of future instruments like the HST will greatly expand H I studies of stars at low latitude and those behind dense clouds, and it will also increase the number of other objects that can be used for Lα studies. For example, only a few Lα absorption measurements have been made against the chromospheric emission from very nearby, late-type stars (189) because with the *IUE* they can be observed to only $\sim$30 pc from the Sun.

Higher order members of the Lyman series (Lβ, Lγ, Lδ, . . .) are in principle accessible to check column densities and, if the higher order lines are not saturated, to obtain velocity information (e.g. 272). Only the *Copernicus* satellite, however, was able to observe substantially shortward of Lα, e.g. to Lβ at 1026 Å, and it will be some time before there is general coverage of these wavelengths again, for the HST is limited to $\lambda > 1060$ Å.

For a number of years there was a discrepancy between the values of $N_H$ derived from Lα absorption and from 21-cm emission measurements made in the same direction at moderate and high galactic latitude (42, 131). In all cases $N_H$(21 cm) was greater than $N_H$(Lα), sometimes by an order of magnitude. Plots of $N_H$(Lα) vs $N_H$(21 cm) showed little if any correlation, even on a log-log scale (224). Blame for the disagreement was variously laid to the poor angular resolution of radio telescopes or to some radiative transfer phenomenon.

The structure of the local ISM and of the Galaxy caused most of the early problems [as suggested by Spitzer & Jenkins (243)]. Stray radiation in the 21-cm observations contributed to the confusion, but it was not the main effect. Lα observations of nearby stars show less H I than 21-cm observations because the Sun is located in a low-density cavity (reviewed in ref. 57); nearly all galactic H I lies behind the nearby stars. It was an unfortunate coincidence that in the region of the Orion Nebula, which was the target of many early studies, most of the gas is also behind the bright stars, so again $N_H$(Lα) $\ll N_H$(21 cm). A bias of this sort is expected in most

ultraviolet/radio comparisons because ultraviolet studies must use sightlines with low reddening, so if there is a substantial amount of H I in a given direction, it must lie behind the stars observed in the UV. Finally, the general thickness and irregularity of the galactic H I layer were not appreciated. Significant amounts of H I can occur many hundreds of parsecs from the galactic plane, so very high $|z|$ stars are needed for an accurate L$\alpha$/21-cm comparison.

The current situation is summarized in Figure 8, where $N_H$(L$\alpha$) is plotted against $N_H$(21 cm) for a selected set of stars. Figure 8 contains all available observations that meet the following criteria (from ref. 123): (*a*) The target stars are of spectral type B2 or earlier, (*b*) the stars are $\gtrsim 30°$ from the galactic plane, (*c*) they are at least 1500 pc above or below the galactic plane, and (*d*) the 21-cm observations are not contaminated by stray radiation. The L$\alpha$ data are from the *Copernicus* and *IUE* satellites; the 21-cm data are from the Green Bank 140-ft telescope (67, 167, 225). The error bars are $\pm 1\sigma$ experimental errors. The agreement between ultraviolet and radio estimates of $N_H$ is excellent and somewhat astonishing, considering that the angular resolutions, experimental techniques, and telescopes differ in all respects. Even the rather coarse 21′ angular resolution of the radio data apparently does not introduce a large error. Within the experimental uncertainties, and given the rather select nature of the target directions, the L$\alpha$ and 21-cm techniques give consistent results.

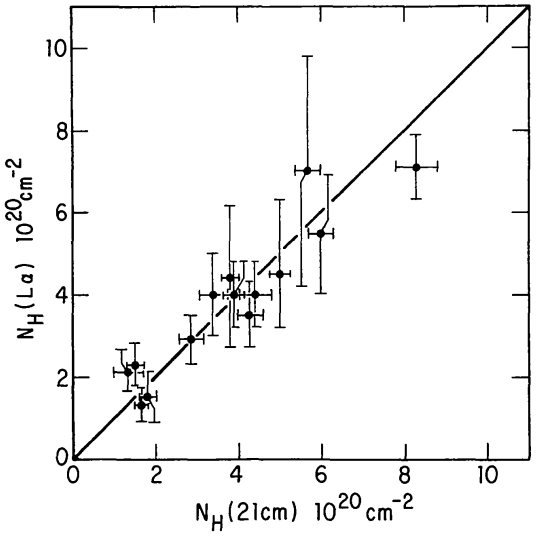


*Figure 8* High-latitude H I column densities derived from radio (21-cm) observations over a 21′ beam compared with column densities derived from UV (L$\alpha$) observations toward very distant stars in the same direction. Error bars are experimental $\pm 1\sigma$ values. The excellent agreement between the two vastly different ways of measuring H I is reassuring and also indicates that there is not very much angular structure in $N_H$ at high latitudes (see also Section 5.2).

# 4. INDIRECT TRACERS OF H I

Alternatives to L$\alpha$ and 21-cm observations give independent estimates of the properties of galactic H I, often over paths that cannot otherwise be studied. This is not a comprehensive account of the relationship between H I and other interstellar species, but rather a summary of some of those that can be used as predictors of H I.

## 4.1 *Spectral Lines*

Interstellar absorption lines from species like Ca, Na, K, and Ti can be used to infer the distribution of H I when variations in excitation and depletion by adsorption on the grains are small. [This topic was recently reviewed by Cowie & Songaila (54; see also 242, 243).] The optical absorption line of Ti II at $\lambda$3384 Å is perhaps the best *qualitative* tracer of H I because it is the dominant ionization stage in H I regions and has an ionization potential almost exactly that of hydrogen. This line has been used for several studies of neutral gas (1, 246). Unfortunately, the depletion of Ti is variable and the line cannot be used for quantitative estimates of $N_{\rm H}$. The gas-phase abundance of Ti II depends so sensitively on physical conditions (because of depletion, the abundance is inversely proportional to the ambient density) that the scale height of Ti II is substantially larger than that of H I (85). Where one sees Ti II there must be neutral hydrogen, but the amount is uncertain. Optical lines of Na I and K I correlate well with $N_{\rm H}$, with perhaps a factor of 2 scatter from star to star, but the slope of the relationship between $N$(Na I) and $N_{\rm H}$ may well be a function of $N_{\rm H}$ (91, 122). The H and K lines of Ca II correlate poorly with hydrogen and, according to Hobbs (122), are the least suitable for most purposes.

A review of techniques of optical and UV spectroscopy can be found in (54). Modern detectors have high-velocity resolution ($\sim$1 km s$^{-1}$) and good sensitivity to lines from clouds with an equivalent H I column density $\gtrsim 10^{19}$ cm$^{-2}$. Detailed component-by-component comparisons between 21-cm, optical, and UV spectra are now being made in a few directions (e.g. 67). This multiwavelength approach will be the pattern of future studies of the ISM.

## 4.2 *Dust*

4.2.1 REDDENING AND EXTINCTION The connection between H I and dust has been studied by making comparisons between $N_{\rm H}$ and reddening $E(B-V)$, or between $N_{\rm H}$ and extinction $A_V$, ever since the detection of the 21-cm line (30, 31, 68, 95, 131, 147, 160, 177, 258). Because of the obvious advantage in measuring the H I and reddening over an identical path, the early radio work was superseded by ultraviolet/optical comparisons (20,

132, 243). These have established that $\langle N_H/E(B-V)\rangle = 6\pm 2 \times 10^{21}\,cm^{-2}$ $mag^{-1}$ for sight lines dominated by neutral atomic gas, in agreement with determinations from other methods (20). Indeed, the small but select group of stars [all of which have known $E(B-V)$ values] used for Figure 8 give this value, including the dispersion, provided that the two stars with a reported $E(B-V) = 0$ are omitted. The existence of anomalies like these two stars has provoked a small but important debate on whether there might not be sight lines that have H I but virtually no reddening (e.g. 119). We sidestep this issue by noting that to an H I observer the scatter in $\langle N_H/E(B-V)\rangle$ is so large, no matter what zero point for reddening is adopted or what correction is made for $H_2$, that reddening must be considered a relatively poor estimator of $N_H$, uncertain by a factor of 2 for any star. It is, however, the only way to get $N_H$ in the direction of the large number of stars that are too cool to be good L$\alpha$ targets (e.g. spectral type A), yet are bright enough to be used for study of Ca, Ti, Na, and other interstellar species. An excess of $E(B-V)$ along a given path is also a signal to check for ionized H II or molecular gas, since a significant amount of dust may reside in these phases.

4.2.2 INFRARED EMISSION The *Infrared Astronomical Satellite* (*IRAS*) detected far-IR emission from all directions of the sky. This satellite was so sensitive that it could measure the dust in an equivalent H I column density of order a few times $10^{19}\,cm^{-2}$ at its longer wave bands of 100 and 60 $\mu$m (reviewed in ref. 11). While the *IRAS* results have been very important for interstellar studies, it seems that interstellar conditions vary so widely that far-IR emission is only a qualitative predictor of galactic H I; it also follows $H_2$, dust associated with H II regions, and the interstellar radiation field (21, 118).

The galactic, diffuse IR emission that *IRAS* measured can be separated into two general components: The dominant one is a relatively smooth background that varies as csc $|b|$. Superimposed on that are large, filamentary "cirrus" features (170). Both components have exact analogs in H I, and some cirrus are seen optically as reflection nebulae (221a). At high galactic latitudes and in the outer Galaxy where molecules are relatively rare, there is a detailed point-by-point correlation between $I$(100 $\mu$m) and $N_H$, but the IR emissivity per H atom varies by a factor of 3 from place to place (21, 251). This is because the far-IR brightness and color depend on the mixture of small and large grains and on their temperature. The grain-size distribution may well vary from place to place depending on the grain creation and destruction processes at work in the local environment (21a), while the interstellar radiation field is a strong function of position (83, 201).

Other anomalies in the H I–IR correlation can be attributed to the presence of significant amounts of molecular hydrogen (often traced by emission in the radio lines of CO) or ionized gas. This has stimulated attempts to compare all convenient dust and gas tracers, an idea that of course predates the *IRAS* survey (e.g. 65). The cirrus clouds appear to be at the transition between primarily molecular and primarily atomic gas; with column densities of 3–5 $\times$ $10^{20}$ cm$^{-2}$ they can barely shield their CO and $H_2$ from photodissociation (see Section 5.3). So neither 21-cm nor CO emission studies give the total gas column density directly, and even with both in hand there are uncertainties in the conversion factor between CO emission intensity and $H_2$ column density. Finally, the gas-to-dust ratio is probably not constant. Variations in the Milky Way have been found from pre-*IRAS* studies (31, 51, 120a), and Schwering (231, pp. 195–252) has shown that it has a different value in the Small Magellanic Cloud.

One of the more exciting questions about the relationship between *IRAS* cirrus and ordinary clouds traced by 21-cm emission is the frequent correspondence between far-IR emission and multiple velocity components in the H I profiles. Often the H I shows highly supersonic velocity discontinuities in the vicinity of cirrus, and anomalous intermediate velocity material is often seen associated with far-IR bright clouds (70, 118). The prototype for this effect is the "Dracula" cloud (in Draco), which has been studied for many years by Mebold and others (182, and references therein; 219a). All these cases suggest enhancement of the far-IR emission behind shocks such as those caused by cloud collisions. On the other hand, the good overall correlation between far-IR and 21-cm emission means that it cannot exclusively be anomalous velocity gas that corresponds to the cirrus, since this gas makes up a fairly small fraction of the total H I on most lines of sight. No 100-$\mu$m emission has been detected from high-velocity H I clouds (274).

## 4.3 *Absorption in the EUV and Soft X-Ray Bands*

Any measurement of the opacity of the ISM at wavelengths between the Lyman limit and the C-band edge (0.28 keV; $\lambda = 44$ Å) can be used to determine the column density of neutral hydrogen, because in this energy range only hydrogen and helium contribute significantly to the absorption cross section (184). At the lower energies, the high H I cross section limits the observations to very near (more precisely, very low $N_H$) objects, but in the soft X-ray bands (for example, near 0.2 keV), the total opacity through the galactic disk at high latitudes may be only $\sim$2. To derive an accurate $N_H$ from these observations corrections must be made for molecular gas along the line of sight and for the neutral helium in any low-excitation H II regions that might be encountered. The background source must also

have a strong EUV or soft X-ray flux and, most importantly, an intrinsic spectrum that is well known, so that the photoelectric absorption can be measured precisely.

The H I density near the Sun is so low that the spectra of a number of white dwarfs have been observed from the near-ultraviolet right through the Lyman limit (124). This is possible only because the stars are nearby, are bright, and have total column densities in their direction $\ll 10^{19}$ cm$^{-2}$. Such targets are rare. Of more general use are estimates of the total $N_H$ from soft X-ray observations of extragalactic sources like active galaxies and quasars. But here the limit is the uncertainty in the "expected" X-ray spectrum. Indeed, the first attempts to solve simultaneously for the X-ray spectral index and the column density of intervening H I for a number of quasars yielded values for $N_H$ that were much too small. It is now recognized that QSOs have complex X-ray spectra, and this makes them of little use as tools for deriving an accurate galactic $N_H$ (see 280). Even for sources that have a simple power-law spectrum, the uncertainty in the $N_H$ derived from current data is relatively large (e.g. 173).

The next generation of X-ray observatories, beginning with *ROSAT*, will measure spectra of many tens of thousands of objects. These will be useful for determining $N_H$ in some situations and will help to identify regions of the sky that have excess X-ray opacity caused by the presence of molecular gas or neutral He in a low-ionization-state H II region. Attenuation of soft X rays by He in the diffuse ionized component, in particular, may be substantial (215). The extragalactic X-ray observations will be an independent complement to the IR observations in disentangling the state of the ISM at high galactic latitudes.

## 4.4 *Gamma Rays*

Surveys of diffuse gamma-ray emission by orbiting observatories such as *SAS-2* and *COS*-B have provided another way of measuring the abundance of interstellar matter, including H I (92a; recently reviewed in ref. 15). Gamma rays with energies in the range of a few hundred to a few thousand MeV are produced mainly by bremsstrahlung of cosmic-ray electrons with energies $\sim$1 GeV and by decay of $\pi^0$ particles produced by collisions of cosmic rays with the ISM. By observing the gamma-ray surface brightness and comparing it with the distribution of interstellar gas, one can deduce the density of cosmic rays as a function of position in the Galaxy (12a, 245a). Conversely, since the galactic nonthermal radio emission gives a good estimate of the cosmic-ray density in this energy range (17, 214), one could derive the total amount of interstellar matter from the gamma-ray brightness. In practice, the most useful approach has been to start from the surveys of 21-cm and CO emission as tracers of the H I and $H_2$,

respectively, and to try to reproduce the observed gamma-ray brightness using various galactic models (247, and references therein).

There are observational and theoretical limitations to this technique. The gamma-ray observations have low angular resolution ($\geq 1°.5$ for *COS-B*), so the survey of diffuse brightness is confusion limited by small sources. Also, large-angle, nearby interstellar structures, like radio Loop I, must be removed (15). In addition, there are uncertainties in interpreting the gamma-ray flux due to our limited understanding of cosmic-ray propagation in the Galaxy, both on small scales (e.g. magnetic reflection from clouds) and large scales (e.g. leakage from the disk). When higher resolution data become available they will give a more detailed picture of both the cosmic-ray distribution in the Galaxy and its interaction with interstellar clouds (13, 16, 17). This should occur this year (1990) with the launch of the *Gamma Ray Observatory* (92b).

It is unlikely that the techniques described in this section will supplant the more direct methods of measuring interstellar H I, but they do serve as an independent check that is especially important in tracing gas not easily measured otherwise, such as molecular hydrogen and the low-density, ionized component.

## 5. THE ORGANIZATION OF INTERSTELLAR H I

There has been a significant change in our understanding of the morphology of galactic H I as new observations have revealed structures on scales ranging from 1 kpc to $\lesssim 100$ AU. With this has also come a breakdown in the rigid distinction between atomic and molecular clouds. The main message of these new data may be that galactic H I cannot be understood unless viewed in conjunction with all other phases of the ISM, both locally and globally.

### 5.1 *Bubbles, Shells, and Supershells*

It has been evident since the early emission studies of Heiles (110) and Verschuur (270) that the most prominent interstellar atomic hydrogen structures are shaped like sheets and filaments, often with velocity gradients and often arranged in shells. The most convincing shells show an empty cavity centered on some velocity $v_0$, two bright "polar caps" at the central position but with velocity offsets $v_0 \pm v_{\rm exp}$, and in between a symmetric change of shell size with velocity, with the largest size at $v_0$ (150). While few shells appear so cleanly in the data, shells or shell fragments are seen throughout the Galaxy with a very broad range of size (for catalogs, see 112, 114, 244). This diversity probably reflects the variety of physical processes that generate the shells. It is possible that the expanding ring of

gas and stars that we call Gould's Belt is a shell viewed from within (40, 161, 193, 222).

Supershells, with diameters of more than a kiloparsec, are often larger than the disk thickness and may open into the halo. Some of these (e.g. the anticenter shell) have so much kinetic energy (some $10^{53}$ ergs) that they have been attributed to the impact of infalling high-velocity clouds on the disk (155, 183, 249, 250). Other supershells can be explained by the combined effect of multiple supernovae in an association (116).

There are a great many shells with diameters of a few hundred parsecs; most of these are probably the old remnants of one or more supernovae that are a few times $10^6$ or even $10^7$ years old. Often these have associated shells of molecular gas and radio continuum emission (108, and references therein; see also 18, 113, 133, 239). Expansion velocities tend to decrease with increasing size, more or less as expected for old supernova remnants, with typical values for $v_{\rm exp}$ being 25 km s$^{-1}$ or less. The oldest shells have $v_{\rm exp}$ as low as 3 km s$^{-1}$, sizes of a few hundred parsecs, and ages of several million years. Younger supernova remnants also show distinct H I shells; the interaction of these remnants with the surrounding medium has been the topic of numerous studies (e.g. 51, 84, 102, 103, 157, 212, 213).

The energy and, more importantly, the accumulated momentum available in stellar winds are sufficient to generate shells with properties nearly identical to those caused by old supernova remnants (276, and references therein). Many H I shells (these in particular are often called "bubbles") have OB associations near their center (e.g. 39, 41, 260). Typically these bubbles are 50 to 150 pc in diameter, and their range of sizes overlaps that of supernova remnants. Many H II regions show prominent H I velocity discontinuities and cavities, which suggest that H I shells are in the process of forming (22, 134, 212, 213, 217, 268). Striking examples are seen in the VLA maps of Orion A, W3, and BG 2107+49 (262–264).

On the smallest scales (1 pc or less), H I is associated with molecular outflows ($v_{\rm exp} \lesssim 120$ km s$^{-1}$) centered on infrared stars in star-forming regions such as NGC 2071 (7, 71, 72, 218). This atomic gas is likely the dissociation product of molecular gas, either behind the shock formed by the outflow on the surrounding molecular cloud or on the inner edge of the photodissociation front around the young stars. Such high-velocity outflows may represent the earliest stages of bubble formation.

High-resolution maps of H I in other galaxies show disks pockmarked with shells, as well as evidence of the systematic infall or outflow of large neutral clouds (26, 27, 221, 259). These, combined with galactic data, have at times led many H I observers to mentally picture most galactic H I as residing in giant structures shaped by a history of local overpressure from stellar winds or supernovae, rather than in a hierarchy of equilibrium

clouds. Evidence for this extreme view, however, is still circumstantial. There is no solid estimate of the fraction of galactic H I that is tied up in bubbles, shells, and supershells or in their old fragments.

## 5.2 *Small-Scale Structure in Atomic Clouds*

Aperture synthesis observations of 21-cm absorption in front of extended background sources almost always detect some structure in the absorption on angular scales as small as the beam size (see, for example, the discussion of VLBI results in Section 2.1.3). These data are clearly telling us something about the internal composition of interstellar clouds. While it may seem that the telescopes must be resolving ever smaller, independent "cloudlets," this model is not satisfactory. For one thing, the covering factor of the absorbing gas parcels must be large, not small, because the angular scale over which absorption is measured does not seem to affect 21-cm absorption line widths or line shapes or derived spin temperatures (199). That is, the statistical properties of H I absorption lines are identical whether the absorption is measured against point-source pulsars or is averaged over several arcminutes (74). Furthermore, H I emission lines do not show the large point-to-point fluctuations that would occur if a substantial fraction of the ISM were concentrated into small cloudlets (128, 129, 158, 167). There are directions where small-scale density fluctuations can be large, such as the vicinity of H II regions and supernova remnants, but this is not the case in more typical regions. In general, no more than 10% of all H I can be in these small-scale structures, and the fraction is usually much smaller on the subparsec scale. Skeptics on this point should study Figure 8 and note the high correlation between $N_{\rm H}$ measured over a 21′ beam and $N_{\rm H}$ measured over the solid angle of a star. Also, the suggestion that broad, 21-cm emission lines are composed of many beam-smeared, narrow-velocity components (271a) is inconsistent with the observation of absorption spectra toward distant stars (e.g. Ti II; 1), which often show broad lines identical to those in 21 cm. Cloudlets cannot be the fundamental form of a significant fraction of interstellar H I.

Nevertheless, aperture synthesis observations do show some variation in 21-cm opacity on all angular scales. One of the most detailed 21-cm observational studies ever done on a single field (136) found H I clouds in a complex of clumps with sizes of 0.5–1 pc and masses of 0.03–0.5 $M_\odot$. The solid-angle covering factor of the clumps is large, so they overlap in front of the background source, although Gaussian decomposition of the absorption spectrum shows these features to be distinct in velocity. About three quarters of the H I, however, is not in these clouds but rather is spread so smoothly across the field on scales $>10'$ that the interferometer could not detect it. Structure on linear scales of 0.1 pc and smaller has

been probed by only a few experiments (60, and references therein; 73, 105), but these also show variations in optical depth of perhaps 20% at a given velocity across a background radio source (see Section 2.1.3).

We believe that the evidence is against large variations in column density on small scales, and that the concept of "cloudlets" is not a useful one in describing most H I. The fluctuations in optical depth that are observed on scales smaller than 1 pc or so most probably arise from turbulence and temperature fluctuations within clouds. This implies that H I clouds are both far from quiescence and far from thermal and dynamic equilibrium.

## 5.3 *The Relation Between Atomic and Molecular Gas*

Molecules require shielding against UV photodissociating radiation; this requires a layer of partially atomic gas whose thickness (column density) depends on the rate of molecule formation, and hence on the space density (265; reviewed in refs. 257b,c). Molecular hydrogen is a significant component of those interstellar clouds that have $N_{\rm H} \gtrsim 5 \times 10^{20}$ cm$^{-2}$ (224a). In low-density environments it is hard to trace the molecular hydrogen column density using the most common tool (millimeter-wave CO emission lines), in part because the shielding of CO is rather different from that of $H_2$ and in part because a total density of about $10^3$ cm$^{-3}$ is needed to keep the collision rate high enough to maintain the 3-mm transition in local thermodynamic equilibrium. Even so, CO emission is detected from some primarily atomic clouds (63, 175, and references therein). Also, OH absorption lines show that molecular cores are present inside clouds that show H I absorption (76, 132a), and larger, primarily molecular clouds have atomic halos (275) or residual cool H I (37, 101).

It is at high latitudes that the various types of atomic and low-mass molecular clouds can best be distinguished. Beginning with the pioneering work of L. Magnani and L. Blitz, high-latitude molecular clouds have been studied in surveys of CO, OH, $C_3H_2$, and other molecules (57a, 173a, 175, 175b, 257a, 281b). The nearby high-latitude clouds have masses of only a few hundred solar masses, much lower than that of the giant molecular clouds in the disk (which can reach $10^6$ $M_\odot$ or more) and lower than such nearby large molecular complexes as Orion and Taurus. Often they are found in the catalog by Lynds (171b) of dust clouds selected as discrete, intermediate-$A_V$ regions on the Palomar Sky Survey.

Observations of CO, CH, and OH can also be used to trace molecules in much lower $A_V$ regions that have been called "translucent molecular clouds" (132a, 175a, 281b), although they are predominantly atomic and have masses of only a few hundred solar masses and $A_V < 1$. Typically, the 21-cm line is in self-absorption in such clouds. Some of the far-IR cirrus clouds correspond to this translucent molecular cloud population,

but most cirrus clouds show no trace of CO or any other radio molecular species, which is not surprising since the sky covering factor of CO-bearing clouds is only about 0.5% (174), whereas cirrus covers almost 10% of the high-latitude sky. Thus, most cirrus clouds are probably diffuse atomic clouds.

The physical conditions in the translucent molecular clouds and the diffuse atomic clouds are very similar; they have densities of 50–100 $cm^{-3}$ and temperatures of 50–100 K. The molecules simply reside in the higher column density regions, where they are shielded from photodissociating UV. Thus, the translucent molecular clouds, and even the Lynds-type clouds at high latitude, may be simply the cores of the larger atomic diffuse clouds. "Core," however, is not the best description, since in fact these shielded regions often have an octopus- or spongelike morphology.

Most of the cool atomic hydrogen at the solar circle and beyond, where the surface density of atomic gas is greater than that of molecular gas (34, 231a), is probably in clouds that are primarily atomic rather than molecular. In the inner Galaxy, where the molecular gas surface density exceeds that of H I, much of the H I may be associated with molecular clouds, either as halos, as a photodissociation product near young stellar associations [as is the case in M51 (252)], or as the low-density substrate for the molecular "mist" suggested by Solomon et al (240). Warm H I, at least half of which is not associated with clouds (50, 162), remains about as abundant in the inner Galaxy as it is in the solar neighborhood.

## 5.4 *Cloud Mass Spectrum*

The range of cloud masses spans more than a factor of $10^6$, from the giant molecular clouds to the diffuse atomic clouds. To measure the interstellar cloud mass spectrum, i.e. the distribution function of cloud masses, different tracers are needed for different types of clouds, and results obtained from these may be difficult to put on the same scale. The problem is that absorption surveys, whether in the 21-cm, optical, or UV lines, give the number of clouds per unit line-of-sight distance (the mean free path) as a function of optical depth, whereas emission surveys (e.g. in CO) give the number of clouds per unit volume (cloud abundance or density) as a function of flux or brightness temperature (86, and references therein; 230a, and references therein). The latter can be converted, at least approximately, into cloud abundance versus mass, and the former into mean free path versus column density, but the issues of cloud cross section and internal density structure still need to be addressed in order to put these kinds of measurements together.

Dickey & Garwood (77) made rough guesses for these quantities to produce the abundance function of Figure 9, which shows the number of

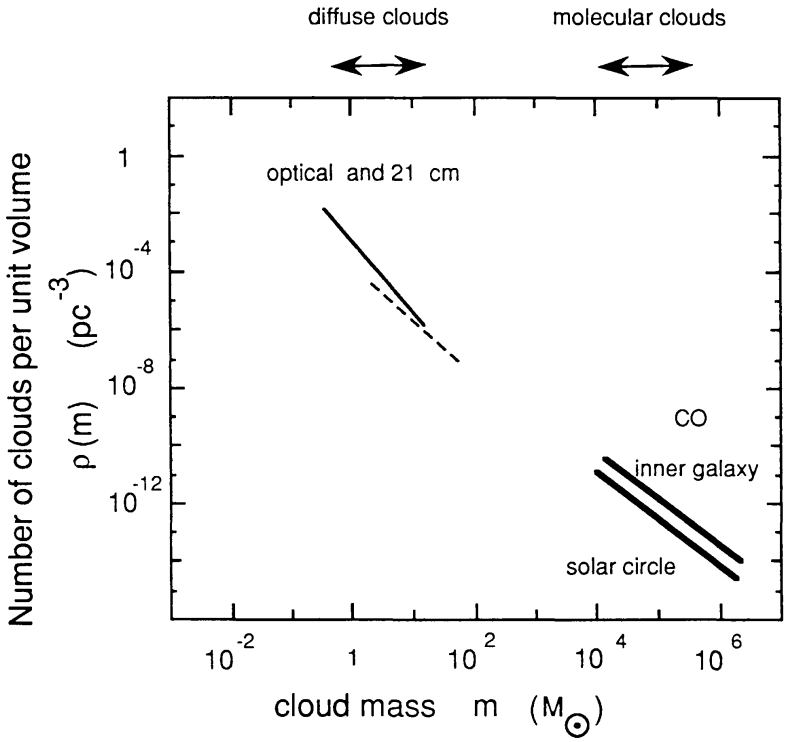


*Figure 9* The "mass spectrum" of interstellar clouds. This figure plots an estimate of the distribution function by mass of clouds, i.e. the number of clouds per unit interstellar volume as a function of cloud mass. Relatively complete inventories of the galactic cloud population are available only over limited ranges of mass. The two solid lines on the right show results from molecular cloud surveys, normalized to give the molecular gas surface density at the solar circle and at the inner Galaxy peak. The solid and dashed lines on the left represent estimates for atomic clouds based on 21-cm absorption surveys and two assumptions for cloud temperatures (77).

clouds per unit volume $\rho(m)$ as a function of cloud mass $m$. Cloud mass is defined so that $2 \times \langle|z|\rangle \times \int \rho(m)\, dm$ gives the surface density of gas in the cloud phase. The mass ranges that are directly observed are indicated; the center of this figure is blank, not because it is difficult to see such clouds (e.g. with masses $10^3\ M_\odot$), but because they are difficult to inventory over a large area owing to incompleteness in the surveys. Also, we do not know the cutoff at the low-mass end, which determines the total mass in clouds if the slope is as steep as it appears among the low-mass clouds detected in optical and 21-cm absorption. In computing this cloud mass spectrum it is important to avoid using cloud sizes, if possible, because observationally, cloud size has only a weak dependence on mass. It must be that cloud sizes are determined by a variety of mechanisms (77, 190).

Our observational knowledge of the cloud mass spectrum is still so rudimentary that it is difficult to know how much theoretical interpretation

of Figure 9 is justified. It is reassuring that the observed slopes for atomic clouds and for molecular clouds are about the same; the slope measured from molecular surveys for clouds in the mass range of a few times $10^4$–$10^6$ $M_\odot$ is about $-1.6$, whereas the slope measured for diffuse clouds with masses 1–10 $M_\odot$ is about $-2.1$. Given that there are roughly equal gas surface densities in the molecular and cool atomic phases, the slope is necessarily near $-2$, which is the critical slope giving an equal-mass contribution from each decade mass range. A simple theory of collisional agglomeration (the "Oort model") predicts a slope of $-1.5$ (94), but the theory has many possible variations depending on the physics of cloud collisions and the velocity distribution of clouds (e.g. 52, 53, 227, and references therein; 236, 283). A slope near $-1.5$ is not necessarily ruled out by the data, at least over mass ranges of several orders of magnitude.

On a more fundamental level, the interpretation of the survey results implicit in Figure 9 does not take account of the hierarchical clustering of interstellar clouds (e.g. 126, 226a). Aggregates of smaller clouds make up larger clouds, all arranged typically on large shells or at least sheets, sometimes punctured by smaller, younger shells or bubbles. In the inner Galaxy, a large fraction of the cool atomic gas may be associated with molecular clouds. This association raises the question of which structures are distinct clouds and which are mere halos, cores, or the substrata of a larger complex. The term cloud, a metaphor drawn from the terrestrial atmosphere, is fraught with such imponderables, which are reflected in the difficulty of objectively delimiting discrete features in emission surveys (176).

## 5.5 *Random Motions*

To measure random velocities (as distinct from the large-scale galactic rotation), either the atomic gas must be clearly associated with an object that has a known distance [e.g. an H II region (232)] or a particular region of *l-v* space must be studied in which the effect of galactic rotation is somehow isolated. Examples of the latter are the lines of sight to the galactic center and the anticenter (151, 211, 230), velocities near the terminator (subcentral point) in the inner Galaxy (151), and high-latitude clouds (58). Results from the various studies have generated some recent controversy and have revealed several surprising properties of interstellar H I.

There is evidence for several kinematic populations of interstellar H I, not counting the high- and intermediate-velocity clouds that are defined empirically as having a velocity well outside the range permitted by galactic rotation (267a). The cloud population studied in absorption has a velocity dispersion of $\sim 7$ km s$^{-1}$ (11a, 58, 230). In emission the dispersion is

somewhat higher for the bulk of the H I, but it depends on the method of analysis and the specific region of the Galaxy being studied (151). The dispersion may increase toward the inner Galaxy. In addition, a component of H I seen in both emission and absorption has a velocity dispersion in the range 15–35 km $s^{-1}$ (3, 232, and references therein), although the amount of gas in this phase was overestimated at first (see 151). Whether this component is distinct from the intermediate-velocity gas, or even from some of the high-velocity gas, is not clear (273). At rms velocities of 15–35 km $s^{-1}$ the velocity distribution is quite symmetric, whereas the higher velocities have a clear preference for infall in a class of high-velocity clouds. There is a predominance of infalling gas at high positive galactic latitudes even at velocities of $-20$ to $-50$ km $s^{-1}$, but this seems to be local to the solar neighborhood (279).

A very interesting result from a study by Kulkarni & Fich (151) is that at high latitudes the kinetic energy $[v^2N(v)]$ per unit velocity in H I is approximately constant from 10 to 70 km $s^{-1}$, i.e. the amount of gas decreases as velocity to the power $-2$ (see also 1). The physical cause of this equipartition of kinetic energy among equal-velocity intervals is not clear.

In addition to these truly random motions, there are systematic departures from galactic rotation associated with galactic structure. A galactic bar or density wave will induce large-scale H I streaming, and a spiral shock pattern can explain many of the velocity anomalies observed in absorption toward H II regions (10, 33, 104a, 232).

## 6. VERTICAL STRUCTURE

### 6.1 *Thickness of the H I Layer*

In recent years there has been renewed interest in measuring and understanding the vertical distribution of H I and other components of the ISM. The concentration of H I to the galactic plane was evident in the earliest observations (195); in the inner Galaxy most of it lies in a layer that has a thickness between half-density points of only about 220 pc. The thickness is approximately constant from $0.4R_0$ to $R_0$, but it decreases to $<100$ pc near the nucleus and increases enormously at $R > R_0$ (171). The vertical density profile $n(z)$ is approximately Gaussian near the plane with a low-density tail to high $z$ (165). The gas lies in a flattened system interior to the solar orbit but is systematically warped in its outer parts (29, 139, 142). A cross section of the Galaxy that illustrates most of these features is given by Burton (34). Recent research has focused on topics like the detailed shape of $n(z)$ and its variation in the Galaxy, the maximum extent of the

neutral layer, and the perennial, provocative question of what holds the whole thing up.

It is necessary to consider UV, optical, and radio data together because each has revealed a different aspect of the vertical structure of H I. The classic Ca II observations of Münch & Zirin (188) showed that there were neutral interstellar clouds up to $z \sim 1$ kpc, a discovery that has been confirmed and broadened through optical and UV measurements of many species (1, 66, 137a, 185a, 225). The 21-cm emission data provide most of the information on vertical structure but are usually dominated by low-$z$ gas; L$\alpha$ studies show a component that is 3 times wider than the main layer deduced from 21-cm data (20). The cumulative effect of these observations has led to a new appreciation of the vertical stratification of the ISM. One can lay out a hierarchy of increasing physical temperature (or ionization state) with increasing scale height that goes from molecular clouds (the species most confined to the plane) through H I and on into the gas traced in highly excited ions like C IV, Si IV, and N V, which extends several kiloparsecs above the disk (225). It is natural to ask if there might also be separate stratified components within the atomic hydrogen itself, and this question has led to attempts to decompose the 21-cm data into populations with separate scale heights, usually in the spirit of the two-phase model (5, 90, 154, 208). Typically, the hotter H I is found to have a scale height of order 1.5 times that of the colder clouds.

The vertical stratification shows dramatically in L$\alpha$/21-cm comparisons toward high-latitude stars, where it is observed that the scale height of H I is usually inversely proportional to the mean density along the line of sight (167). This implies that dense clouds are in the thinnest layer and probably accounts for the general difference between L$\alpha$ and 21-cm scale heights. A recent L$\alpha$ study (225) toward stars chosen to have "the lowest attainable color excess and H I column densities per kiloparsec" measured values of $N_{\rm H}$ that are consistent with a single exponential distribution with $n(0) = 0.1$ cm$^{-3}$ and a scale height of 800 pc. This particular result is a product of the target selection and may not pertain to any interstellar H I component, but it again illustrates the composite nature of the vertical structure and reminds us that along some sight lines, often spanning many kiloparsecs, integrated properties vary by a factor of 5 from global averages. Indeed, density fluctuations are often many times larger than the mean at all altitudes, as one might guess from Figure 7. Moderate-density H I clouds are found many hundreds of parsecs to several kiloparsecs from the plane, and parts of H I supershells extend to $z > 600$ pc (112, 114, 165, 238). In all, the layer is not very tidy, and it looks like a smooth function of $z$ only when averaged over large volumes of the Galaxy (see, for example, 45).

In recent years there has been special interest in the highest $z$ H I, which lies in the lower galactic halo at $|z| > 500$ pc. This medium extends far beyond the H I disk. It may regulate the evolution of supernovae and supershells (172), may contain much of the kinetic energy of the ISM (151), and may be connected with events high in the galactic halo via a galactic fountain (23, 125, 192). Halo H I is difficult to measure in the 21-cm line because of blending with the much brighter disk gas and contamination of profiles by stray radiation. The most conspicuous neutral components are clouds whose velocities are peculiar enough to make them stand out against the rest of the ISM.

Such objects are common locally, and a prime example is the intermediate-velocity H I that covers much of the northern galactic polar regions at column densities occasionally as high as a few times $10^{20}$ cm$^{-2}$ (80b, 279). It is falling toward the galactic plane at about $-50$ km s$^{-1}$. Absorption-line studies toward halo stars have bracketed its vertical distance between 340 and 760 pc, which implies that it has a mass of $10^5\ M_\odot$ (66). This cloud (or, more likely, "sheet") contains $\sim 10\%$ of the H I mass in the solar neighborhood and is probably connected with the evolution of the local bubble (57). It is a nearby example of a general galactic process that may produce most high-velocity clouds (23).

This leads to the question of whether halo H I is all in structures either rising or falling, or whether there is also a truly diffuse, static medium. Studies of general halo H I are not yet able to give a definitive answer, but we feel that the observations point toward a halo in which the neutral gas is mainly composed of discrete structures, such as intermediate-velocity clouds or the fragments of supershells that are so evident in Figure 7.

## 6.2 *Average* n(z)

Recent analyses have suggested the following general form for the vertical density function $n(z)$: In the innermost few kiloparsecs, inside the radius of the galactic bulge but outside of the galactic nucleus, the layer is extremely thin and is approximated by a single Gaussian with a $\sigma \lesssim 70$ pc; in the outermost regions, beyond the solar circle at $R > R_0$, the layer flares dramatically and nearly linearly, reaching $\langle z^2 \rangle^{1/2} \gtrsim 3$ kpc (34, 82, 121, 149, 165). Gas in the outer Galaxy is distributed in a complicated multicomponent layer. Faint emission extends very far from the main concentrations, reminiscent of the "thick envelopes" of H I that are seen around some galaxies (e.g. 221).

From radii of perhaps 4–8 kpc, the layer has approximately constant average properties (although, as noted above, with very large fluctuations). This is the most studied part of the galactic disk. Our "best estimate" of $n(z)$ over this region is given in Figure 10. It is a combination of two

Gaussians, of central densities 0.395 and 0.107 $cm^{-3}$ and FWHMs of 212 and 530 pc, and an exponential with $n(0) = 0.064$ $cm^{-3}$ and a scale height of 403 pc. The distribution has a FWHM of 230 pc, a central density of 0.57 $cm^{-3}$, and $N_H = 6.2 \times 10^{20}$ $cm^{-2}$ through a full disk. This function was derived from the data given by Lockman (165) scaled to $R_0 = 8.5$ kpc and corrected for the undercounted H I at low $z$ in that study by increasing the central density of the narrowest component.

For comparison, Figure 10 also shows other density profiles that have been derived for galactic H I. The UV data (Savage & Massa) were obtained along very low $N_H$ lines of sight, which accounts for the low $n(0)$ although not necessarily for the large scale height, while the earlier radio data did not have sufficient sensitivity or vertical coverage to catch the faint tail. Descriptions of the central layer, however, have been remarkably consistent among radio observers (see also 45, 140), and in all, the various differences displayed in Figure 10 probably reflect the diversity of the neutral ISM.

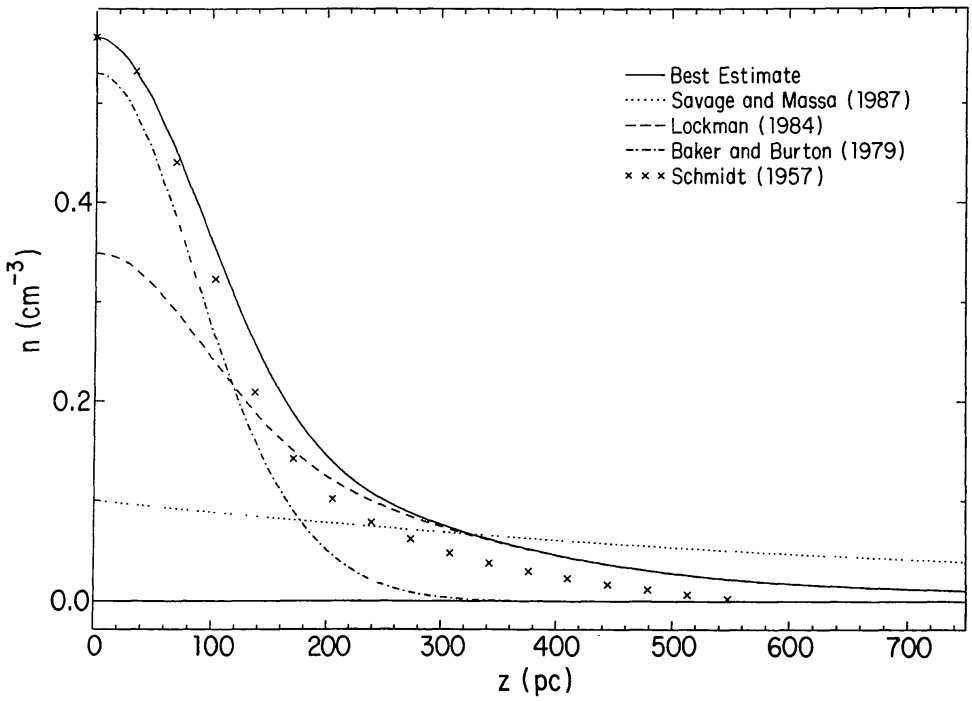


*Figure 10* Recent estimates of the vertical density distribution of galactic H I in the range $0.4\ R_0 \lesssim R \lesssim R_0$. All are based on 21-cm data (5, 165), except for the Savage & Massa (225) curve, which comes from L$\alpha$ observations of a sample of exceptionally low $N_H$ lines of sight. The curve marked "Best Estimate" is what we believe to be the most likely distribution and is discussed in the text. For comparison, the crosses show the values $n(z)$ derived by Schmidt (228) in 1957 after they are adjusted to a central density of 0.57 $cm^{-3}$. All curves have been scaled to $R_0 = 8.5$ kpc.

## 6.3 *Support of the Layer*

The kinetic temperature of H I is far too low to support it to its observed height against the galactic potential. It must be held up by turbulent pressure (random motion of H I clouds) or by nonthermal pressure from cosmic rays and magnetic fields. Models of global equilibrium have been suggested that incorporate all three forms of support (4, 14, 55, 56, 96, 138, 196; reviewed by 284); most of the models are dynamically unstable. It is not clear that cosmic rays or magnetic fields have a vertical pressure gradient large enough to provide the needed support, but we do not discuss the possibilities here [see Spitzer's article in this volume (242a) for more on this topic]. Instead, it is interesting to consider the vertical distribution that would result just from the H I motions that are measured in 21-cm emission profiles. Examination of high-latitude 21-cm spectra in the solar neighborhood shows that there is enough kinetic energy in H I motion to maintain a layer to a FWHM of 350 pc, and also that about 15% of the H I could be in a component with a scale height of $\sim$500 pc (151, 169). This distribution is reasonably like the measured one (Figure 10) given the large uncertainties, so we consider it possible that cloud-cloud or bulk motion rather than nonthermal pressure supports the neutral ISM, at least in the solar neighborhood.

An item that puzzled Oort in 1962 (195), and which is still unresolved, is the apparent constancy of the layer's thickness from $0.4R_0$ to $\sim R_0$, despite the change in the gravitational potential by a factor of several over this range (19, 152; but see ref. 146 for a different opinion). Beyond the solar circle the layer thickens to an extent consistent with a decrease in the gravitational potential, but there is no corresponding narrowing interior to the solar circle. Suggestions that increased cosmic-ray and magnetic pressure exactly compensate the change in gravity seem artificial. No other solution to the dilemma is apparent unless one is prepared to consider the entire ISM, rather than just the atomic component, as one entity that is in vertical balance. In that case, the overall layer does narrow substantially in the inner Galaxy because molecular gas, which increasingly dominates the total surface density at small $R$, is much more confined to the plane than the H I.

## 6.4 *Deviations From a Plane*

6.4.1 CORRUGATIONS When H I observations were used to redefine the galactic coordinate system it was noticed that there was a residual "waviness" of the inner-Galaxy H I layer about the new galactic plane (106). Since then, there have been several attempts to determine if the waviness has some large-scale pattern, for in some areas the deviations of the average

$z$ from zero seem to be tantalizingly regular, as if they are manifestations of ordered "corrugations" that have an amplitude of a few tens of parsecs. A similar, though perhaps not identical, effect appears in H II regions and other constituents of the ISM (164, 202–204, 241). The form of these distortions is not at all certain, for it is difficult to disentangle galactic structures except in special directions, and it is even harder to follow individual H I features for any distance in the Galaxy. An unambiguous observational picture of the inner Galaxy corrugations might best be done in species that are less abundant and therefore less confused than H I.

6.4.2 THE WARP The H I warp is one of the most striking but least understood features of the Galaxy. Recent research has been reviewed by Burton (34). The warp has an integral-sign shape; its line of nodes is close to the Sun-center line and does not change significantly with $R$. The warp begins just outside of the solar circle and extends to the Galaxy's edge; it reaches an altitude of 4 kpc in the north, whereas in the south it seems to turn back toward the plane after reaching only $\sim -1.5$ kpc. But these numbers do not do justice to the extent of the warp, for with the combined flaring of the layer and its vertical displacement it is easily seen to latitudes of $\sim 30^\circ$ in some directions (82). At its outermost edge the warp is fluted as if by a higher frequency vertical distortion (249). Many other spiral galaxies show even more extreme large-scale warps (25).

Accurate measurement of H I in the warp is an observational challenge because of the high angular resolution, sensitivity, and freedom from stray radiation that are required (166). Our knowledge of the warp, and thus of the ultimate extent and size of the Galaxy, is certain to increase in the coming years as better observational and theoretical tools are used to study it.

6.4.3 CYLINDRICAL ROTATION Is it possible that when the gas layer is significantly and systematically displaced from a simple plane, the rotational motion of the H I deviates from strict corotation with the motion at $z = 0$ and has full three-dimensional structure? Is gas in the galactic warp, for example, rotating as if it were firmly fixed to the extension of the galactic plane that lies a scale height below it? As of now, these questions can be answered only for special subsets of galactic H I. It seems likely that H I in the inner Galaxy, for example, is corotating to at least 1 kpc, while high-velocity clouds, though they have some component of galactic rotation, are following paths of their own (98, 99, 165). Also, there are hints that some of the highest scale-height ions (C IV) are lagging behind galactic rotation (225). Determination of the rotation curve away from the galactic plane is critical in establishing a distance to gas in the outermost parts of the Galaxy and the galactic halo (179, 223), but it will

probably be done with indirect tracers of H I, such as optical and UV absorption lines, rather than with measurements of H I itself. The importance of the assumption of corotation should not be underestimated when analyzing velocities in the halo and outer Galaxy.

## ACKNOWLEDGMENTS

We are grateful to numerous colleagues for useful conversations and advice. In particular, we thank Tom Bania, Hans Bloemen, Leo Blitz, Don Cox, Carl Heiles, George Helou, Lew Hobbs, Harvey Liszt, Phil Maloney, Dan McCammon, Ed Salpeter, Blair Savage, John Scalo, Lyman Spitzer, and Barry Turner for their helpful suggestions. We are also very grateful for the expert assistance of Terry Thibeault, Executive Secretary in the Astronomy Department at the University of Minnesota. JMD wishes to thank the Nederlandse Wetenschappelijk Onderzoek (ZWO) and the hospitality of the Sterrewacht Leiden, where much of this work was done. This work was supported in part by the National Science Foundation under grant 87-22990 to the University of Minnesota. The National Radio Astronomy Observatory is operated by Associated Universities, Inc., under agreement with the National Science Foundation.

*Literature Cited*

1. Albert, C. E. 1983. *Ap. J.* 272: 509–39
2. Alferova, Z. A., Venger, A. P., Gosachinskij, I. V., Grashev, V. G., Egorova, T. M., et al. 1987. *Astrofiz. Issled. Izv. Spets. Astrofiz. Obs.* 24: 93–107
3. Anantharamaiah, K. R., Radhakrishnan, V., Shaver, P. A. 1984. *Astron. Astrophys.* 138: 131–39
4. Badhwar, G. D., Stephens, S. A. 1977. *Ap. J.* 212: 494–506
5. Baker, P. L., Burton, W. B. 1975. *Ap. J.* 198: 281–97
6. Baker, P. L., Burton, W. B. 1979. *Astron. Astrophys. Suppl.* 35: 129–52
7. Bally, J., Stark, A. A. 1983. *Ap. J. Lett.* 266: L61–64
8. Bania, T. M. 1983. *Astron. J.* 88: 1222–27
9. Bania, T. M., Lockman, F. J. 1984. *Ap. J. Suppl.* 54: 513–45
10. Bash, F. N., Leisawitz, D. 1985. *Astron. Astrophys.* 145: 127–34
11. Beichman, C. A. 1987. *Annu. Rev. Astron. Astrophys.* 25: 521–63
11a. Belfort, P., Crovisier, J. 1984. *Astron. Astrophys.* 136: 368–70
12. Bertaux, J. 1984. In *The Local Interstellar Medium, IAU Colloq. No. 81. NASA Conf. Publ. 2345*, ed. Y. Kondo, F. C. Bruhweiler, B. D. Savage, pp. 3–23. Greenbelt, Md: NASA
12a. Bignami, G. F., Fichtel, C. E. 1974. *Ap. J. Lett.* 189: L65–67
13. Bloemen, J. B. G. M., Strong, A. W., Blitz, L., Cohen, R. S., Dame, T. M., et al. 1986. *Astron. Astrophys.* 154: 25–41
14. Bloemen, J. B. G. M. 1987. *Ap. J.* 322: 694–705
15. Bloemen, H. (J. B. G. M.) 1989. *Annu. Rev. Astron. Astrophys.* 27: 469–516
16. Bloemen, J. B. G. M., Bennett, K., Bignami, G. F., Blitz, L., Caraveo, P. A., et al. 1984. *Astron. Astrophys.* 135: 12–22
17. Bloemen, J. B. G. M., Reich, P., Reich, W., Schlickeiser, R. 1988. *Astron. Astrophys.* 204: 88–100
18. Bochkarev, N. G. 1984. *Sov. Astron. Lett.* 10: 76–78
19. Bohigas, J. 1988. *Astron. Astrophys.* 205: 257–66
20. Bohlin, R. C., Savage, B. D., Drake, J. F. 1978. *Ap. J.* 224: 132–42
21. Boulanger, F., Perault, M. 1988. *Ap. J.* 330: 964–85
21a. Boulanger, F., Falgarone, E., Puget, J. L., Helou, G. 1990. *Ap. J.* In press

22. Braunsfurth, E. 1983. *Astron. Astrophys.* 117: 297–304
23. Bregman, J. N. 1980. *Ap. J.* 236: 587–91
24. Bregman, J. D., Troland, T. H., Forster, J. R., Schwarz, U. J., Goss, W. M., Heiles, C. 1983. *Astron. Astrophys.* 118: 157–62
25. Briggs, F. H. 1990. *Ap. J.* 352: 15–29
26. Brinks, E., Braun, R., Unger, S. W. 1989. In *Structure and Dynamics of the Interstellar Medium, IAU Colloq. No. 120*, ed. G. Tenorio-Tagle, M. Moles, J. Melnick, pp. 524–29. Berlin: Springer-Verlag
27. Brinks, E., Bajaja, E. 1986. *Astron. Astrophys.* 169: 14–42
28. Brown, R. L., Liszt, H. S. 1984. *Annu. Rev. Astron. Astrophys.* 22: 223–65
29. Burke, B. F. 1967. *Astron. J.* 63: 90
30. Burstein, D., Heiles, C. 1978. *Ap. J.* 225: 40–55
31. Burstein, D., Heiles, C. 1984. *Ap. J. Suppl.* 54: 33–79
32. Burton, W. B. 1966. *Bull. Astron. Inst. Neth.* 18: 247–55
33. Burton, W. B. 1976. *Annu. Rev. Astron. Astrophys.* 14: 275–306
34. Burton, W. B. 1988. In *Galactic and Extragalactic Radio Astronomy*, ed. K. Kellermann, G. L. Verschuur, pp. 295–358. New York: Springer-Verlag
35. Burton, W. B., Deul, E. R. 1987. In *The Galaxy*, ed. G. Gilmore, B. Carswell, pp. 141–72. Dordrecht: Reidel
36. Burton, W. B., Gordon, M. A. 1978. *Astron. Astrophys.* 63: 7–27
37. Burton, W. B., Liszt, H. S., Baker, P. L. 1978. *Ap. J. Lett.* 219: L67–72
38. Burton, W. B., te Lintel Hekkert, P. 1986. *Astron. Astrophys. Suppl.* 65: 427–63
39. Cappa de Nicolau, C. E., Niemela, V. S. 1984. *Astron. J.* 89: 1398–1403
40. Cappa de Nicolau, C. E., Niemela, V. S., Arnal, E. M. 1986. *Astron. J.* 92: 1414–19
41. Cappa de Nicolau, C. E., Poppel, W. G. L. 1986. *Astron. Astrophys.* 164: 274–99
42. Carruthers, G. R. 1969. *Ap. J. Lett.* 156: L97–100
43. Carruthers, G. R. 1970. *Space Sci. Rev.* 10: 459–82
44. Caswell, J. L., Murray, J. D., Roger, R. S., Cole, D. J., Cooke, D. J. 1975. *Astron. Astrophys.* 45: 239–58
45. Celnik, W., Rohlfs, K., Braunsfurth, E. 1979. *Astron. Astrophys.* 76: 24–34
45a. Christiansen, W. N., Hogbom, J. A. 1985. *Radio Telescopes*. Cambridge: Univ. Press. 2nd ed.
46. Clark, B. G. 1965. *Ap. J.* 142: 1398–1422
47. Clark, B. G., Radhakrishnan, V., Wilson, R. W. 1962. *Ap. J.* 135: 151–74
48. Cleary, M. N., Heiles, C., Haslam, C. G. T. 1979. *Astron. Astrophys. Suppl.* 36: 95–127
49. Clifton, T. R., Frail, D. A., Kulkarni, S. R., Weisberg, J. M. 1988. *Ap. J.* 333: 332–40
50. Colgan, S. W. J., Salpeter, E. E., Terzian, Y. 1988. *Ap. J.* 328: 275–98
51. Colomb, F. R., Dubner, G. M., Giacani, E. B. 1984. *Astron. Astrophys.* 130: 294–300
52. Cowie, L. L. 1980. *Ap. J.* 236: 868–79
53. Cowie, L. L. 1981. *Ap. J.* 245: 66–71
54. Cowie, L. L., Songaila, A. 1986. *Annu. Rev. Astron. Astrophys.* 24: 499–535
55. Cox, D. P. 1986. In *Model Nebulae*, ed. D. P. Pequignot, pp. 11–22. Meudon, Fr: Obs. Paris
56. Cox, D. P. 1987. See Roger & Landecker 1987, pp. 73–90
57. Cox, D. P., Reynolds, R. J. 1987. *Annu. Rev. Astron. Astrophys.* 25: 303–44
57a. Cox, P., Gusten, R., Henkel, C. 1988. *Astron. Astrophys.* 206: 108–16
58. Crovisier, J. 1978. *Astron. Astrophys.* 70: 43–50
59. Crovisier, J., Dickey, J. M. 1983. *Astron. Astrophys.* 122: 282–96
60. Crovisier, J., Dickey, J. M., Kazes, I. 1985. *Astron. Astrophys.* 146: 223–34
61. Crovisier, J., Kazes, I., Aubry, D. 1978. *Astron. Astrophys. Suppl.* 32: 205–82
62. Crovisier, J., Kazes, I., Aubry, D. 1980. *Astron. Astrophys. Suppl.* 41: 229–84
63. Crovisier, J., Kazes, I., Brillet, J. 1984. *Astron. Astrophys.* 138: 237–45
64. Crutcher, R. M., Kazes, I., Troland, T. H. 1987. *Astron. Astrophys.* 181: 119–26
65. Dall'Oglio, G., de Bernardis, P., Masi, S., Melchiorri, F., Moreno, G., Trabalza, R. 1985. *Ap. J.* 289: 609–12
66. Danly, L. 1989. *Ap. J.* 342: 785–806
67. Danly, L., Savage, B. D., Lockman, F. J., Meade, M. R. 1990. *Ap. J.* In press
68. Davies, R. D. 1956. *MNRAS* 116: 443–52
69. Davies, R. D., Cummings, E. R. 1975. *MNRAS* 170: 95–113
70. Deul, E., Burton, W. B. 1990. *Astron. Astrophys.* In press
71. Dewdney, P. E., Roger, R. S. 1982. *Ap. J.* 255: 564–76
72. Dewdney, P. E., Roger, R. S. 1986. *Ap. J.* 307: 275–85
73. Diamond, P. J., Goss, W. M., Romney, J. D., Booth, R. S., Kalberla, P. M. W., Mebold, U. 1989. *Ap. J.* 347: 302–6
74. Dickey, J. M., Weisberg, J. M., Rankin, J. M., Boriakoff, V. 1981. *Astron. Astrophys.* 101: 332–41

75. Dickey, J. M., Benson, J. M. 1982. *Astron. J.* 87: 278–305
76. Dickey, J. M., Crovisier, J., Kazes, I. 1981. *Astron. Astrophys.* 98: 271–85
77. Dickey, J. M., Garwood, R. W. 1989. *Ap. J.* 341: 201–7
78. Dickey, J. M., Kulkarni, S. R., van Gorkom, J. H., Heiles, C. E. 1983. *Ap. J. Suppl.* 53: 591–621
79. Dickey, J. M., Salpeter, E. E., Terzian, Y. 1977. *Ap. J. Lett.* 211: L77–81
80. Dickey, J. M., Salpeter, E. E., Terzian, Y. 1978. *Ap. J. Suppl.* 36: 77–114
80a. Dickey, J. M. 1990. In *The Interstellar Medium in External Galaxies*, ed. J. M. Shull, H. A. Thronson. Dordrecht: Kluwer. In press
80b. Dieter, N. H. 1964. *Astron. J.* 69: 288–93
81. Dieter, N. H., Welch, W. J., Romney, J. D. 1976. *Ap. J. Lett.* 206: L113–15
82. Diplas, A., Savage, B. D. 1990. *Ap. J.* In press
83. Draine, B. T., Anderson, N. 1985. *Ap. J.* 292: 494–99
84. Dubner, G. M., Colomb, F. R., Giacani, E. B. 1986. *Astron. J.* 91: 343–53
85. Edgar, R. J., Savage, B. D. 1989. *Ap. J.* 340: 762–74
86. Elmegreen, B. G. 1987. In *Interstellar Processes*, ed. D. J. Hollenbach, H. A. Thronson, Jr., pp. 259–80. Dordrecht: Reidel
87. Elmegreen, D. M., Elmegreen, B. G. 1987. *Ap. J.* 314: 3–9
88. Elvis, M., Lockman, F. J., Wilkes, B. J. 1989. *Astron. J.* 97: 777–82
89. Ewen, H. I., Purcell, E. M. 1951. *Nature* 168: 350–56
90. Falgarone, E., Lequeux, J. 1973. *Astron. Astrophys.* 25: 253–60
91. Ferlet, R., Vidal-Majar, A., Gry, C. 1985. *Ap. J.* 298: 838–43
92. Ferriere, K. M., Zweibel, E. G., Shull, J. M. 1988. *Ap. J.* 332: 984–94
92a. Fichtel, C. E., Hartman, R. C., Kniffen, D. A., Thompson, D. J., Bignami, G. F., et al. 1975. *Ap. J.* 198: 163–82
92b. Fichtel, C. E. 1989. In *Large Scale Surveys of the Sky. Proc. NRAO Workshop No. 20*, ed. J. J. Condon, F. J. Lockman, pp. 143–60. Green Bank, W. Va: NRAO
92c. Fiedler, R. L., Dennison, B., Johnston, K. J., Hewish, A. 1987. *Nature* 326: 675–78
93. Field, G. B. 1958. *Proc. Inst. Radio Eng.* 46: 240–50
94. Field, G. B., Saslaw, W. C. 1965. *Ap. J.* 142: 568–83
95. Fong, R., Jones, L. R., Shanks, T., Stevenson, P. R. F., Strong, A. W., et al. 1987. *MNRAS* 224: 1059–72
96. Fuchs, B., Thielheim, K. O. 1979. *Ap. J.* 227: 801–7
97. Garwood, R. W., Dickey, J. M. 1989. *Ap. J.* 338: 841–61
98. Giovanelli, R. 1980. *Astron. J.* 85: 1155–81
99. Giovanelli, R. 1986. In *Gaseous Halos of Galaxies. Proc. NRAO Workshop No. 12*, ed. J. N. Bregman, F. J. Lockman, pp. 99–114. Green Bank, W. Va: NRAO
100. Goss, W. M., Radhakrishnan, V., Brooks, J. W., Murray, J. D. 1972. *Ap. J. Suppl.* 24: 123–59
101. Goss, W. M., Retallack, D. S., Felli, M., Shaver, P. A. 1983. *Astron. Astrophys.* 117: 115–26
102. Gosachinskij, I. V., Khersonskij, V. K. 1987. *Astrophysics* 26: 40–44
103. Gosachinskij, I. V., Khersonskij, V. K. 1987. *Sov. Astron. AJ* 31: 621–23
104. Greisen, E. W. 1973. *Ap. J.* 184: 363–90
104a. Greisen, E. W., Lockman, F. J. 1979. *Ap. J.* 228: 740–47
105. Greisen, E. W., Liszt, H. S. 1986. *Ap. J.* 303: 702–17
106. Gum, C. S., Kerr, F. J., Westerhout, G. 1960. *MNRAS* 121: 132–49
107. Hagen, J. P., Lilley, A. E., McClain, E. F. 1955. *Ap. J.* 122: 361–75
108. Handa, T., Sofue, Y., Reich, W., Furst, E., Suwa, I., Fukui, Y. 1986. *Publ. Astron. Soc. Jpn.* 38: 361–78
109. Heeschen, D. J. 1955. *Ap. J.* 121: 569–84
110. Heiles, C. 1967. *Ap. J. Suppl.* 15: 97–130
111. Heiles, C. 1974. In *Galactic Radio Astronomy, IAU Symp. No. 60*, ed. F. J. Kerr, S. C. Simonson, III, pp. 13–44. Dordrecht: Reidel
112. Heiles, C. 1979. *Ap. J.* 229: 533–44
113. Heiles, C. 1980. *Ap. J.* 235: 833–39
114. Heiles, C. 1984. *Ap. J. Suppl.* 55: 585–95
115. Heiles, C. 1987. In *Interstellar Processes*, ed. D. J. Hollenbach, H. A. Thronson, Jr., pp. 171–92. Dordrecht: Reidel
116. Heiles, C. 1987. *Ap. J.* 315: 555–66
116a. Heiles, C. 1988. *Ap. J.* 324: 321–30
117. Heiles, C. 1989. *Ap. J.* 336: 808–21
118. Heiles, C., Reach, W. T., Koo, B.-C. 1988. *Ap. J.* 332: 313–27
119. Heiles, C., Stark, A. A., Kulkarni, S. 1981. *Ap. J. Lett.* 247: L73–76
120. Heiles, C., Wrixon, G. T. 1976. In *Methods of Experimental Physics*, ed. M. L. Meeks, 12C: 58–77. New York: Academic

120a. Helou, G. 1989. In *Interstellar Dust, IAU Symp. No. 135*, ed. L. J. Allamandola, A. G. G. M. Tielens, pp. 285–301. Dordrecht: Kluwer
121. Henderson, A. P., Jackson, P. D., Kerr, F. J. 1982. *Ap. J.* 263: 116–22
122. Hobbs, L. M. 1974. *Ap. J.* 191: 381–93
123. Hobbs, L. M., Morgan, W. W., Albert, C. E., Lockman, F. J. 1985. *Ap. J.* 263: 690–95
124. Holberg, J. B. 1984. In *The Local Interstellar Medium, IAU Colloq. No. 81. NASA Conf. Publ. No. 2345*, ed. Y. Kondo, A. C. Bruhweiler, B. D. Savage, pp. 41–94. Greenbelt, Md: NASA
125. Houck, J. C., Bregman, J. D. 1990. *Ap. J.* 352: 506–21
126. Houlahan, P., Scalo, J. 1990. *Ap. J. Suppl.* 72: 133–52
127. Hughes, M. P., Thompson, A. R., Colvin, R. S. 1971. *Ap. J. Suppl.* 23: 323–70
128. Jahoda, K., McCammon, D., Dickey, J. M., Lockman, F. J. 1985. *Ap. J.* 290: 229–37
129. Jahoda, K., McCammon, D., Lockman, F. J. 1986. *Ap. J. Lett.* 311: L57–61
130. Jahoda, K., Lockman, F. J., McCammon, D. 1990. *Ap. J.* 354: In press
131. Jenkins, E. B. 1970. In *Ultraviolet Stellar Spectra and Related Ground-Based Observations, IAU Symp. No. 36*, ed. L. Houziaux, H. E. Butler, pp. 281–301. Dordrecht: Reidel
132. Jenkins, E. B., Savage, B. D. 1974. *Ap. J.* 187: 243–55
132a. Jenniskens, P. M. M., Wouterloot, J. G. A. 1990. *Astron. Astrophys.* 227: 553–62
133. Jonas, J. L. 1986. *MNRAS* 219: 1–12
134. Joncas, G., Dewdney, P. E., Higgs, L. A., Roy, J. R. 1985. *Ap. J.* 298: 596–613
135. Kalberla, P. M. W., Mebold, U., Reich, W. 1980. *Astron. Astrophys.* 82: 275–86
136. Kalberla, P. M. W., Schwarz, U. J., Goss, W. M. 1985. *Astron. Astrophys.* 144: 27–36
137. Kazes, I., Aubry, D. 1973. *Astron. Astrophys.* 22: 413–20
137a. Keenan, F. P., Dufton, P. L., McKeith, C. D., Blades, J. C. 1983. *MNRAS* 203: 963–75
138. Kellman, S. A. 1972. *Ap. J.* 175: 353–62
139. Kerr, F. J. 1958. *Rev. Mod. Phys.* 30: 924–25
140. Kerr, F. J. 1969. *Annu. Rev. Astron. Astrophys.* 7: 39–66
141. Kerr, F. J., Bowers, P. F., Jackson, P. D., Kerr, M. 1986. *Astron. Astrophys. Suppl.* 66: 373–504
142. Kerr, F. J., Hindman, J. V., Carpenter, M. S. 1957. *Nature* 180: 677–79
143. Kerr, F. J., Westerhout, G. 1965. In *Galactic Structure* (*Stars and Stellar Systems*, Vol. 5), ed. A. Blaauw, M. Schmidt, pp. 167–202. Chicago: Univ. Chicago Press
144. Knapp, G. R. 1974. *Astron. J.* 79: 527–40
145. Knapp, G. R. 1975. *Astron. J.* 80: 111–16
146. Knapp, G. R. 1987. *Publ. Astron. Soc. Pac.* 99: 1134–43
147. Knude, J. 1981. *Astron. Astrophys.* 98: 74–80
148. Kuchar, T. A., Bania, T. M. 1990. *Ap. J.* 352: 192–206
149. Kulkarni, S. R., Blitz, L., Heiles, C. 1982. *Ap. J. Lett.* 259: L63–66
150. Kulkarni, S. R., Dickey, J. M., Heiles, C. 1985. *Ap. J.* 291: 716–21
151. Kulkarni, S. R., Fich, M. 1985. *Ap. J.* 289: 792–802
152. Kulkarni, S. R., Heiles, C. 1987. In *Interstellar Processes*, ed. D. J. Hollenbach, H. A. Thronson, Jr., pp. 87–122. Dordrecht: Reidel
153. Kulkarni, S. R., Heiles, C. 1988. In *Galactic and Extragalactic Radio Astronomy*, ed. K. I. Kellerman, G. L. Verschuur, pp. 95–153. New York: Springer-Verlag
154. Kulkarni, S. R., Heiles, C., van Gorkom, J., Dickey, J. M. 1984. In *The Local Interstellar Medium, IAU Colloq. No. 81. NASA Conf. Publ. No. 2345*, ed. Y. Kondo, F. C. Bruhweiler, B. D. Savage, pp. 269–73. Greenbelt, Md: NASA
155. Kulkarni, S. R., Mathieu, R. 1986. *Astrophys. Space Sci.* 118: 531–33
156. Kulkarni, S. R., Turner, K., Heiles, C., Dickey, J. M. 1985. *Ap. J. Suppl.* 57: 631–42
157. Landecker, T. L., Roger, R. S., Dewdney, P. E. 1982. *Astron. J.* 87: 1379–89
158. Lazareff, B. 1975. *Astron. Astrophys.* 42: 25–35
159. Levinson, F. H., Brown, R. L. 1980. *Ap. J.* 242: 416–23
160. Lilley, A. E. 1955. *Ap. J.* 121: 559–68
161. Lindblad, P. O., Grape, K., Sandqvist, Aa., Schober, J. 1973. *Astron. Astrophys.* 24: 309–12
162. Liszt, H. S. 1983. *Ap. J.* 275: 163–74
163. Liszt, H. S. 1988. In *Galactic and Extragalactic Radio Astronomy*, ed. K. Kellermann, G. L. Verschuur, pp. 359–80. New York: Springer-Verlag

164. Lockman, F. J. 1977. *Astron. J.* 82: 408–13
165. Lockman, F. J. 1984. *Ap. J.* 283: 90–97
166. Lockman, F. J. 1988. In *The Outer Galaxy*, ed. L. Blitz, F. J. Lockman, pp. 79–88. New York: Springer-Verlag
167. Lockman, F. J., Hobbs, L. M., Shull, J. M. 1986. *Ap. J.* 301: 380–94
168. Lockman, F. J., Jahoda, K., McCammon, D. 1986. *Ap. J.* 302: 432–49
169. Lockman, F. J., Gehman, C. 1990. *Ap. J.* In press
170. Low, F. J., Beintema, D. A., Gautier, T. N., Gillett, F. C., Beichman, C. A., et al. 1984. *Ap. J. Lett.* 278: L19–22
171. Lozinskaya, T. A., Kardashev, N. S. 1963. *Sov. Astron. AJ* 7: 161–66
171b. Lynds, B. T. 1962. *Ap. J. Suppl.* 7: 1–52
172. MacLow, M. H., McCray, R. 1988. *Ap. J.* 324: 776–85
173. Madejski, G. M., Schwartz, D. A. 1989. In *BL Lac Objects: 10 Years After*, ed. L. Maraschi, T. Maccaro, M.-H. Ulrich, pp. 267–80. Heidelberg: Springer-Verlag
173a. Magnani, L., Blitz, L., Mundi, L. 1985. *Ap. J.* 295: 402–21
174. Magnani, L., Lada, E. A., Blitz, L. 1986. *Ap. J.* 301: 395–97
175. Magnani, L., Blitz, L., Wouterloot, J. G. A. 1988. *Ap. J.* 326: 909–23
175a. Magnani, L., Lada, E. A., Sandell, G., Blitz, L. 1989. *Ap. J.* 339: 244–57
175b. Magnani, L., Siskind, L. 1990. *Ap. J.* In press
176. Maloney, P. 1990. *Ap. J.* In press
177. Massa, D., Savage, B. D., Fitzpatrick, E. L. 1983. *Ap. J.* 266: 662–83
177a. McCammon, D., Sanders, W. T. 1990. *Annu. Rev. Astron. Astrophys.* 28: 657–88
178. McCutcheon, W. H., Shuter, W. L. H., Booth, R. S. 1978. *MNRAS* 185: 755–69
179. McGee, R. X., Newton, L. M., Morton, D. C. 1983. *MNRAS* 205: 1191–1205
180. Mebold, U., Hills, D. L. 1975. *Astron. Astrophys.* 42: 187–94
181. Mebold, U., Winnberg, A., Kalberla, P. M. W., Goss, W. M. 1982. *Astron. Astrophys.* 115: 223–41
182. Mebold, U., Cernicharo, J., Velden, L., Reif, K., Crezelius, C., Goerigk, W. 1985. *Astron. Astrophys.* 151: 427–34
183. Mirabel, I. F. 1982. *Ap. J.* 246: 112–19
184. Morrison, R., McCammon, D. 1983. *Ap. J.* 270: 119–22
185. Morton, D. C. 1967. *Ap. J.* 147: 1017–24
185a. Morton, D. C., Blades, J. C. 1986. *MNRAS* 220: 927–48
186. Muller, C. A. 1959. In *Paris Symp. Radio Astron.*, ed. R. N. Bracewell, pp. 360–65. Stanford, Calif: Stanford Univ. Press
187. Muller, C. A., Oort, J. H. 1951. *Nature* 168: 357–58
188. Münch, G., Zirin, H. 1961. *Ap. J.* 133: 11–28
189. Murthy, J., Henry, R. C., Moos, H. W., Landsman, W. B., Linsky, J. L., et al. 1987. *Ap. J.* 315: 675–86
190. Myers, P. C. 1987. In *Interstellar Processes*, ed. D. J. Hollenbach, H. A. Thronson, Jr., pp. 71–86. Dordrecht: Reidel
191. Myers, P. C., Goodman, A. A. 1988. *Ap. J.* 329: 392–405
192. Norman, C. A., Ikeuchi, S. 1989. *Ap. J.* 345: 372–83
193. Olano, C. A., Poppel, W. G. L. 1987. *Astron. Astrophys.* 179: 202–18
194. Oort, J. H. 1955. In *Vistas in Astronomy*, ed. A. Beer, 1: 607–16. London: Pergamon
195. Oort, J. H. 1962. In *The Distribution and Motion of Interstellar Matter in Galaxies*, ed. L. Woltjer, pp. 3–22, 71–77. New York: Benjamin
196. Parker, E. N. 1966. *Ap. J.* 145: 811–33
197. Payne, H. E., Dickey, J. M., Salpeter, E. E., Terzian, Y. 1978. *Ap. J. Lett.* 221: L95–98
198. Payne, H. E., Salpeter, E. E., Terzian, Y. 1982. *Ap. J. Suppl.* 48: 199–218
199. Payne, H. E., Salpeter, E. E., Terzian, Y. 1983. *Ap. J.* 272: 540–50
200. Peters, W. C., Bash, F. N. 1987. *Ap. J.* 317: 646–52
201. Puget, J. L., Legerl, A., Boulanger, F. 1985. *Astron. Astrophys. Lett.* 142: L19–22
202. Quiroga, R. J. 1974. *Astrophys. Space Sci.* 27: 323–42
203. Quiroga, R. J. 1977. *Astrophys. Space Sci.* 50: 281–310
204. Quiroga, R. J., Schlosser, W. 1977. *Astron. Astrophys.* 57: 455–59
205. Radhakrishnan, V. 1960. *Publ. Astron. Soc. Pac.* 72: 296–302
206. Radhakrishnan, V. 1974. In *Galactic Radio Astronomy, IAU Symp. No. 60*, ed. F. J. Kerr, S. C. Simonson, III, pp. 3–12. Dordrecht: Reidel
207. Radhakrishnan, V., Brooks, J. W., Goss, W. M., Murray, J. D., Schwarz, U. J. 1972. *Ap. J. Suppl.* 24: 1–14
208. Radhakrishnan, V., Goss, W. M. 1972. *Ap. J. Suppl.* 24: 161–66
209. Radhakrishnan, V., Goss, W. M., Murray, J. D., Brooks, J. W. 1972. *Ap. J. Suppl.* 24: 49–121
210. Radhakrishnan, V., Murray, J. D., Lockhart, P., Whittle, R. P. J. 1972. *Ap. J. Suppl.* 24: 15–47

211. Radhakrishnan, V., Sarma, N. V. G. 1980. *Astron. Astrophys.* 85: 249–51
212. Read, P. L. 1980. *MNRAS* 192: 11–32
213. Read, P. L. 1980. *MNRAS* 193: 487–94
214. Reich, P., Reich, W. 1988. *Ap. J. Suppl.* 74: 7–23
215. Reynolds, R. J. 1989. *Ap. J. Lett.* 339: L29–32
216. Roger, R. S., Caswell, J. L., Murray, J. D., Cole, D. J., Cooke, D. J. 1978. *MNRAS* 182: 209–18
217. Roger, R. S., Irwin, J. A. 1982. *Ap. J.* 256: 127–38
217a. Roger, R. S., Landecker, T. L., eds. 1987. *Supernova Remnants and the Interstellar Medium. Proc. IAU Colloq. No. 101.* Cambridge: Univ. Press
218. Roger, R. S., Pedlar, A. 1981. *Astron. Astrophys.* 94: 238–50
219. Rohlfs, K., Braunsfurth, E., Mebold, U. 1972. *Astron. J.* 77: 711–17
219a. Rohlfs, R., Herbstmeier, U., Mebold, U., Fink, U. 1990. *Astron. Astrophys.* In press
220. Sancisi, R. 1971. *Astron. Astrophys.* 12: 323–31
221. Sancisi, R. 1988. In *QSO Absorption Lines*, ed. J. C. Blades, D. Turnsheck, C. A. Norman, pp. 241–55. Cambridge: Univ. Press
221a. Sandage, A. 1976. *Astron. J.* 81: 954–57
222. Sandquist, Aa., Tomboulides, H., Lindblad, P. O. 1988. *Astron. Astrophys.* 205: 225–34
223. Savage, B. D., de Boer, K. S. 1979. *Ap. J. Lett.* 230: L77–82
224. Savage, B. D., Jenkins, E. B. 1972. *Ap. J.* 172: 491–522
224a. Savage, B. D., Bohlin, R. C., Drake, J. F., Budich, W. 1977. *Ap. J.* 216: 291–307
225. Savage, B. D., Massa, D. 1987. *Ap. J.* 314: 380–96
226. Savage, B. D., Panek, R. J. 1974. *Ap. J.* 191: 659–74
226a. Scalo, J. 1990. In *Physical Processes in Fragmentation and Star Formation*, ed. R. Capuzzo-Dolcetta, C. Chiosi, A. DiFazio. Dordrecht: Kluwer. In press
227. Scalo, J. M., Struck-Marcel, C. 1986. *Ap. J.* 301: 77–82
228. Schmidt, M. 1957. *Bull. Astron. Inst. Neth.* 13: 247–68
229. Schwarz, U. J., Troland, T. H., Albinson, J. S., Bregman, J. D., Goss, W. M., Heiles, C. 1986. *Ap. J.* 301: 320–30
230. Schwarz, U. J., Ekers, R. D., Goss, W. M. 1982. *Astron. Astrophys.* 110: 100–4
231. Schwering, P. B. W. 1989. PhD thesis. Rijksuniv. Leiden, Neth.
231a. Scoville, N. Z., Saunders, D. B. 1987. In *Interstellar Processes*, ed. D. J. Hollenbach, H. A. Thronson, Jr., pp. 21–50. Dordrecht: Reidel
232. Shaver, P. A., Radhakrishnan, V., Anantharamaiah, K. R., Retallack, D. S., Wamsteker, W., Danks, A. C. 1982. *Astron. Astrophys.* 106: 105–8
233. Shull, J. M., Van Steenberg, M. E. 1985. *Ap. J.* 294: 599–614
234. Shuter, W. L. H., Dickman, R. L., Klatt, C. 1987. *Ap. J. Lett.* 322: L103–8
235. Shuter, W. L. H., Verschuur, G. L. 1964. *MNRAS* 127: 387–404
236. Shaya, E. J., Federman, S. R. 1987. *Ap. J.* 319: 76–83
237. Silverglate, P., Terzian, Y. 1978. *Astron. J.* 83: 1412–16
238. Smith, G. P. 1963. *Bull. Astron. Inst. Neth.* 17: 203–8
239. Sofue, Y., Nakai, N. 1983. *Astron. Astrophys. Suppl.* 53: 57–70
240. Solomon, P. M., Rivolo, A. R., Barrett, J., Yahil, A. 1987. *Ap. J.* 319: 730–41
241. Spicker, J., Feitzinger, J. V. 1986. *Astron. Astrophys.* 163: 43–55
242. Spitzer, L. 1985. *Ap. J. Lett.* 290: L21–24
242a. Spitzer, L. Jr. 1990. *Annu. Rev. Astron. Astrophys.* 28: 71–101
243. Spitzer, L. Jr., Jenkins, E. B. 1975. *Annu. Rev. Astron. Astrophys.* 13: 133–64
244. Stacy, J. G., Jackson, P. D. 1982. *Astron. Astrophys. Suppl.* 50: 377–422
245. Stark, A. A., Bally, J., Linke, R. A., Heiles, C. 1990. In press
245a. Stecker, F. W., Solomon, P. M., Scoville, N. Z., Ryter, C. E. 1975. *Ap. J.* 201: 90–97
246. Stokes, G. M. 1978. *Ap. J. Suppl.* 36: 115–41
247. Strong, A. W., Bloemen, J. B. G. M., Dame, T. M., Grenier, I. A., Hermsen, W. 1988. *Astron. Astrophys.* 207: 1–15
248. Sullivan, W. T. 1984. *The Early Years of Radio Astronomy*. Cambridge: Univ. Press
249. Tenorio-Tagle, G., Franco, J., Bodenheimer, P., Różyczka, M. 1987. *Astron. Astrophys.* 179: 219–30
250. Tenorio-Tagle, G. 1980. *Astron. Astrophys.* 88: 61–65
251. Terebey, S., Fich, M. 1986. *Ap. J. Lett.* 309: L73–77
252. Tilanus, R. P. J., Allen, R. J. 1989. *Ap. J. Lett.* 339: L57–62
253. Troland, T. H., Crutcher, R. M., Heiles, C. 1985. *Ap. J.* 298: 808–17
254. Troland, T. H., Heiles, C. 1982. *Ap. J.* 252: 179–92

255. Troland, T. H., Heiles, C. 1982. *Ap. J. Lett.* 260: L19–22
256. Troland, T. H., Heiles, C. 1986. *Ap. J.* 301: 339–45
257. Troland, T. H., Heiles, C., Goss, W. M. 1989. *Ap. J.* 337: 342–54
257a. Turner, B. E., Rickard, L. J, Xu, L.-P. 1989. *Ap. J.* 344: 292–305
257b. Turner, B. E. 1988. In *Galactic and Extragalactic Radio Astronomy*, ed. K. Kellermann, G. L. Verschuur, pp. 154–99. New York: Springer-Verlag
257c. Turner, B. E., Ziurys, L. M. 1988. In *Galactic and Extragalactic Radio Astronomy*, ed. K. Kellermann, G. L. Verschuur, pp. 200–54. New York: Springer-Verlag
258. van de Hulst, H. C., Muller, C. A., Oort, J. H. 1954. *Bull. Astron. Inst. Neth.* 12: 117–49
259. van der Hulst, T., Sancisi, R. 1988. *Astron. J.* 95: 1354–59
260. van der Bij, M. D. P., Arnal, E. M. 1986. *Astrophys. Lett.* 25: 119–25
261. van der Werf, P. P., Goss, W. M., Vanden Bout, P. A. 1988. *Astron. Astrophys.* 201: 311–26
262. van der Werf, P. P., Goss, W. M. 1989. *Astron. Astrophys.* 224: 209–24
263. van der Werf, P. P., Goss, W. M. 1990. *Astron. Astrophys.* In press
264. van der Werf, P. P., Dewdney, P. E., Goss, W. M., Vanden Bout, P. A. 1989. *Astron. Astrophys.* 216: 215–29
265. van Dishoeck, E. F., Black, J. H. 1988. *Ap. J.* 334: 771–802
266. van Gorkom, J. H., Ekers, R. D. 1985. In *Synthesis Imaging*, ed. R. A. Perley, F. R. Schwab, A. H. Bridle, pp. 177–87. Green Bank, W. Va: NRAO
267. van Woerden, H., Takakubo, K., Braes, L. L. 1962. *Bull. Astron. Inst. Neth.* 16: 321–60
267a. van Woerden, H., Schwarz, U. J., Hulsbosch, A. N. M. 1985. In *The Milky Way Galaxy, IAU Symp. No. 106*, ed. H. van Woerden, R. J. Allen, W. B. Burton, pp. 387–408. Dordrecht: Reidel
268. Venger, A. P., Gosachinskij, I. V., Grachev, V. G., Egorova, T. M., Ryzhkov, N. F., et al. 1984. *Astrophys. Space Sci.* 107: 271–87
269. Verschuur, G. L. 1969. *Ap. J.* 156: 861–74
270. Verschuur, G. L. 1970. *Astron. J.* 75: 687–94
271. Verschuur, G. L. 1989. *Ap. J.* 339: 163–70
271a. Verschuur, G. L., Schmelz, J. T. 1989. *Astron. J.* 98: 267–78
272. Vidal-Majar, A., Ferlet, R., Laurent, C., York, D. G. 1982. *Ap. J.* 260: 128–40
273. Wakker, B. P. 1990. *Astron. Astrophys.* In press
274. Wakker, B. P., Boulanger, F. 1986. *Astron. Astrophys.* 170: 84–90
275. Wannier, P. G., Lichten, S. M., Morris, M. 1983. *Ap. J.* 268: 727–38
276. Weaver, R., McCray, R., Castor, J. 1977. *Ap. J.* 218: 377–95
277. Weaver, R., Williams, D. R. W. 1973. *Astron. Astrophys. Suppl.* 8: 1–503
278. Weisberg, J. M., Boriakoff, V., Rankin, J. M. 1987. *Astron. Astrophys.* 186: 307–11
279. Wesselius, P. R., Fejes, I. 1973. *Astron. Astrophys.* 24: 15–34
280. Wilkes, B. J., Elvis, M. 1987. *Ap. J.* 323: 243–62
281. Williams, D. R. W. 1973. *Astron. Astrophys.* 28: 309–11
281a. Wolszczan, A., Cordes, J. M. 1989. *Ap. J. Lett.* 320: L35–39
281b. Wouterloot, J. G. A. 1981. PhD thesis. Rijksuniv, Leiden, Neth.
282. Wrixon, G. T., Heiles, C. 1972. *Astron. Astrophys.* 15: 444–49
283. Wyse, R. F. G. 1986. *Ap. J. Lett.* 311: L41–45
284. Zweibel, E. G. 1987. In *Interstellar Processes*, ed. D. J. Hollenbach, H. A. Thronson, Jr., pp. 195–221. Dordrecht: Reidel